NASA/TM—2005-213625

Materials Chemistry Issues in the Development of a Single-Crystal Solar/Thermal Refractive Secondary Concentrator

Nathan S. Jacobson
Glenn Research Center, Cleveland, Ohio

Robert C. Biering
Analex Corporation, Brook Park, Ohio

May 2005

The NASA STI Program Office . . . in Profile

Since its founding, NASA has been dedicated to the advancement of aeronautics and space science. The NASA Scientific and Technical Information (STI) Program Office plays a key part in helping NASA maintain this important role.

The NASA STI Program Office is operated by Langley Research Center, the Lead Center for NASA's scientific and technical information. The NASA STI Program Office provides access to the NASA STI Database, the largest collection of aeronautical and space science STI in the world. The Program Office is also NASA's institutional mechanism for disseminating the results of its research and development activities. These results are published by NASA in the NASA STI Report Series, which includes the following report types:

- TECHNICAL PUBLICATION. Reports of completed research or a major significant phase of research that present the results of NASA programs and include extensive data or theoretical analysis. Includes compilations of significant scientific and technical data and information deemed to be of continuing reference value. NASA's counterpart of peer-reviewed formal professional papers but has less stringent limitations on manuscript length and extent of graphic presentations.

- TECHNICAL MEMORANDUM. Scientific and technical findings that are preliminary or of specialized interest, e.g., quick release reports, working papers, and bibliographies that contain minimal annotation. Does not contain extensive analysis.

- CONTRACTOR REPORT. Scientific and technical findings by NASA-sponsored contractors and grantees.

- CONFERENCE PUBLICATION. Collected papers from scientific and technical conferences, symposia, seminars, or other meetings sponsored or cosponsored by NASA.

- SPECIAL PUBLICATION. Scientific, technical, or historical information from NASA programs, projects, and missions, often concerned with subjects having substantial public interest.

- TECHNICAL TRANSLATION. English-language translations of foreign scientific and technical material pertinent to NASA's mission.

Specialized services that complement the STI Program Office's diverse offerings include creating custom thesauri, building customized databases, organizing and publishing research results . . . even providing videos.

For more information about the NASA STI Program Office, see the following:

- Access the NASA STI Program Home Page at ***http://www.sti.nasa.gov***

- E-mail your question via the Internet to help@sti.nasa.gov

- Fax your question to the NASA Access Help Desk at 301–621–0134

- Telephone the NASA Access Help Desk at 301–621–0390

- Write to:
  NASA Access Help Desk
  NASA Center for AeroSpace Information
  7121 Standard Drive
  Hanover, MD 21076

NASA/TM—2005-213625

Materials Chemistry Issues in the Development of a Single-Crystal Solar/Thermal Refractive Secondary Concentrator

Nathan S. Jacobson
Glenn Research Center, Cleveland, Ohio

Robert C. Biering
Analex Corporation, Brook Park, Ohio

National Aeronautics and
Space Administration

Glenn Research Center

May 2005

Acknowledgments

It is a pleasure to acknowledge Donald Humphrey, QSS Group, Inc., for the hot press runs and testing of the insulation materials. Assistance from the Analytical Science Group, Materials Division, NASA Glenn Research Center is also appreciated.

This report is a formal draft or working paper, intended to solicit comments and ideas from a technical peer group.

This report contains preliminary findings, subject to revision as analysis proceeds.

Available from

NASA Center for Aerospace Information
7121 Standard Drive
Hanover, MD 21076

National Technical Information Service
5285 Port Royal Road
Springfield, VA 22100

Available electronically at http://gltrs.grc.nasa.gov

Materials Chemistry Issues in the Development of a Single-Crystal Solar/Thermal Refractive Secondary Concentrator

Nathan S. Jacobson
National Aeronautics and Space Administration
Glenn Research Center
Cleveland, Ohio 44135

Robert C. Biering
Analex Corporation
Brook Park, Ohio 44142

Abstract

The proposed solar/thermal Refractive Secondary Concentrator (RSC) is an advanced concept for converting sunlight to useful energy. A translucent crystal concentrates and transmits energy to a heat exchanger, which in turn heats a propellant gas, working gas of a dynamic power system, or a thermopile (ref. 1). Materials are the limiting issue in such a system. Central is the durability of the crystal, which must maintain the required chemical, physical/optical, and mechanical properties as it is heated and cooled. This report summarizes available data to date on the materials issues with this system. We focus on the current leading candidate materials, which are sapphire (Al_2O_3) for higher temperatures and silica (SiO_2) for lower temperatures. We use data from thermochemical calculations; laboratory coupon tests with silica and sapphire; and system tests with sapphire. The required chemical properties include low-vapor pressure and interfacial stability with supporting structural materials. Optical properties such as transmittance and index of refraction must be maintained. Thermomechanical stability is a major challenge for a large, single crystal ceramic and has been discussed in another report (ref. 2). In addition to the crystal, other materials in the proposed system include refractory metals (Nb, Ta, Mo, W, and Re), carbon (C), and high-temperature ceramic insulation. The major issue here is low levels of oxygen, which lead to volatile refractory metal oxides and rapid consumption of the refractory metal. Interfacial reactions between the ceramic crystal and refractory metal are also discussed. Finally, high-temperature ceramic insulating materials are also likely to be used in this system. Outgassing is a major issue for these materials. The products of outgassing are typically reactive with the refractory metals and must be minimized.

1. Introduction

The proposed solar/thermal Refractive Secondary Concentrator (RSC) is an advanced concept for converting sunlight to useful energy (refs. 1 to 6). A large mirror (primary) reflects sunlight to a refracting crystal (secondary) which both concentrates and transmits energy. Figure 1 shows a diagram of the secondary refractor system and figure 2 illustrates the concept. In the cone shaped region of the RSC, the light is concentrated and passed to the faceted region via total internal reflection. The faceted region radiates the energy to the heat exchanger. The advantages of this approach have been discussed in detail in the reports (refs. 1, 3 to 6). The use of a RSC yields extremely high solar concentration ratios (CR) which cannot be achieved with a primary concentrator alone.

This general approach of utilizing a RSC has been developed for terrestrial applications (refs. 7 to 9). Similar shapes have been designed that use refraction and total internal reflection to achieve a high CR. These designs utilize a silica crystal.

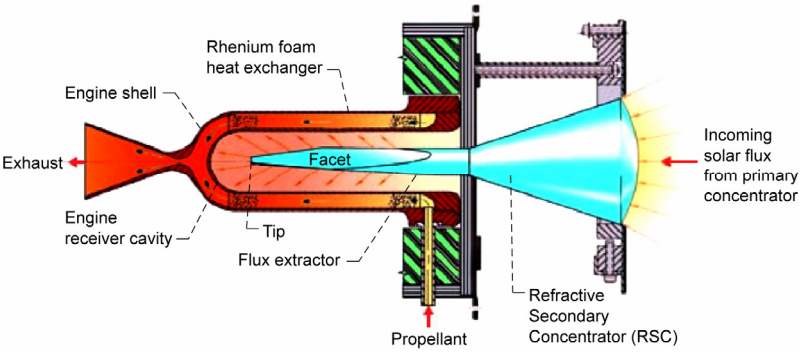

Figrue 1.—Schematic of the solar/thermal RSC engine, primary concentrator not shown (ref. 1).

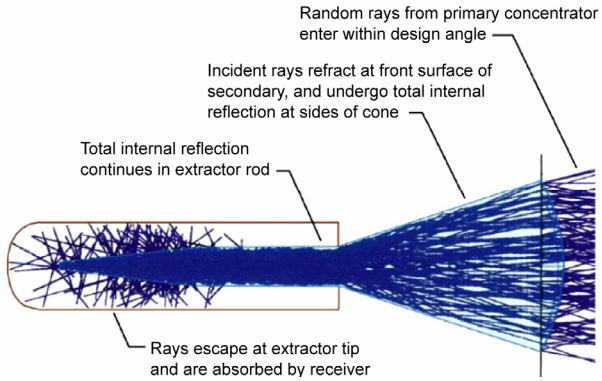

Figure 2.—Diagram illustrating the concept of the refractive secondary concentrator (ref. 2).

Clearly there are a number of strict requirements to fabricate the engine shown in figure 1. Many of these involve selection/development of the proper materials. As shown in figure 1 the system consists of an oxide crystal, refractory metal parts, and ceramic insulation. Most important is the crystal. Concentration limits increase with the square of refractive index (ref. 2), so a high refractive index is desirable. The crystal must maintain optical properties to high temperatures and transmit wavelengths of sunlight (~300 to 2000 nm). Figure 3 shows the transmission of sapphire and silica together with the solar spectrum and the xenon lamp spectrum, which was used in testing. Note that sapphire and silica transmit well across these wavelengths.

Earlier reports have suggested yttria stabilized zirconia ($YO_{1.5}$-ZrO_2), sapphire (Al_2O_3), magnesia (MgO) (ref. 3), and fused silica (SiO_2) (refs. 7 and 8) as candidate crystals. Zirconia can be eliminated due to darkening at high temperatures under reducing conditions. Magnesia can be eliminated due to its high vapor pressure. Therefore we will focus on sapphire and silica. Figure 4 is a photo of the sapphire crystal. There are probably other crystals which can meet the optical requirements, however the development of these crystals is yet another research area. Many of the issues discussed here are general and apply to all possible crystals.

This report is a detailed discussion on these materials challenges. The emphasis here will be on chemical issues; mechanical issues are covered in another report (ref. 2). This report discusses calculations of thermochemical stability, laboratory coupon scale tests, and the results and analyses from two full scale tests with a sapphire crystal. From these we present a view on the thermochemical stability of the two leading crystal candidates—sapphire and fused silica, together with other system construction materials including carbon, niobium, tantalum, molybdenum, tantalum, and rhenium. Thermochemical stability of the insulating ceramic materials will also be discussed.

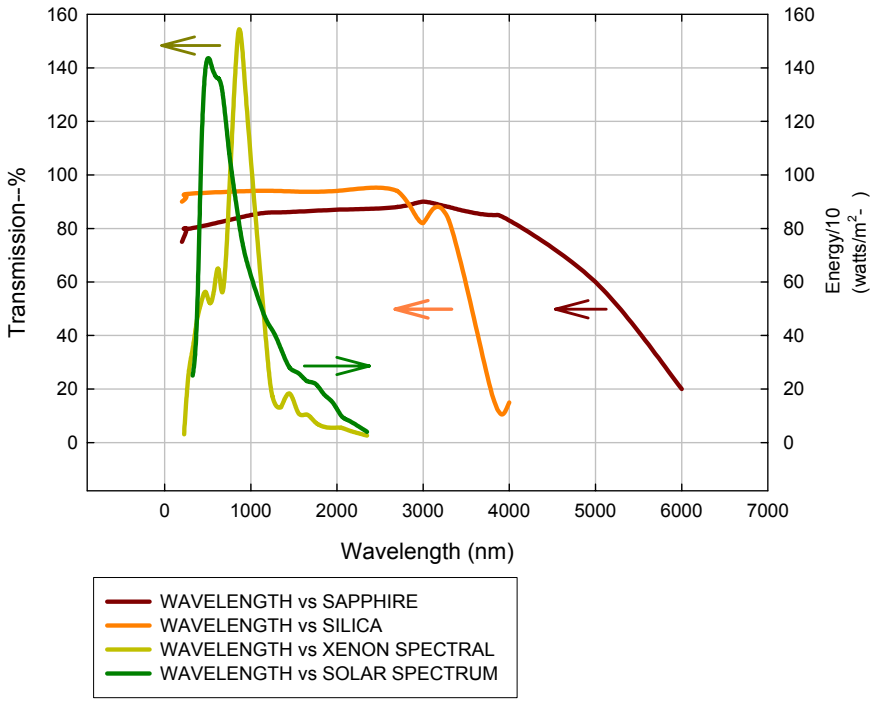

Figure 3.—Transmission versus wavelength for silica and sapphire. The solar spectrum is plotted in energy units, the xenon lamp spectrum is plotted as percent of the total energy at a particular wavelength.

Figure 4.—Photograph of the sapphire crystal.

2. Experimental

2.1 Thermochemical Calculations

Thermochemical calculations were done with the FactSage Computer Code (ref. 10). This code uses a free energy minimization routine to determine stable equilibrium products. It was used to address the following issues:

(1) Vaporization of the candidate crystals.
(2) Reaction of the RSC holder materials with trace amounts of oxygen.
(3) Reaction of the RSC holder materials with the candidate crystals.

2.2 Laboratory Tests

In order to test material compatibility, several vacuum hot press (Oxy-Gon FR-200, Epsom, NH) experiments were done. A refractory metal or carbon was pressed against sapphire. The following heat schedule was followed:

Vacuum at ~10^{-6} torr
Room temperature to 250 °C in 0.5 hr
250 to 1700 °C in 1.5 hr
Hold at 1700 °C for 2 hr at 250 PSIG
1700 °C to room temperature in 2 hr

Graphite rams were used for the carbon/sapphire run and molybdenum rams with a boron nitride (BN) lubricant were used for the molybdenum/sapphire run.

In addition some of the ceramic insulation materials were tested for general behavior in a vacuum at high temperatures, using the furnace of the vacuum hot press. It was found these materials outgassed significantly.

2.3 Full Scale Solar/Thermal Vacuum Tank Tests With a Sapphire Crystal RSC

Three tests were conducted with a sapphire crystal RSC. These were done in the Glenn Research Center Tank 6 Solar Thermal Vacuum Facility. This facility has been described in detail elsewhere (refs. 5 and 6) and consists of a large cryo-pumped vacuum tank (68 ft long by 25 ft diameter) with nine 32 kW xenon lamps which provide 1.2 suns at the primary concentrator. The tank layout and test setup are shown schematically in figure 5(a) to (c). Two types of primary concentrators were used—a fixed disk (shown in fig. 5(a)) and an inflatable concentrator.

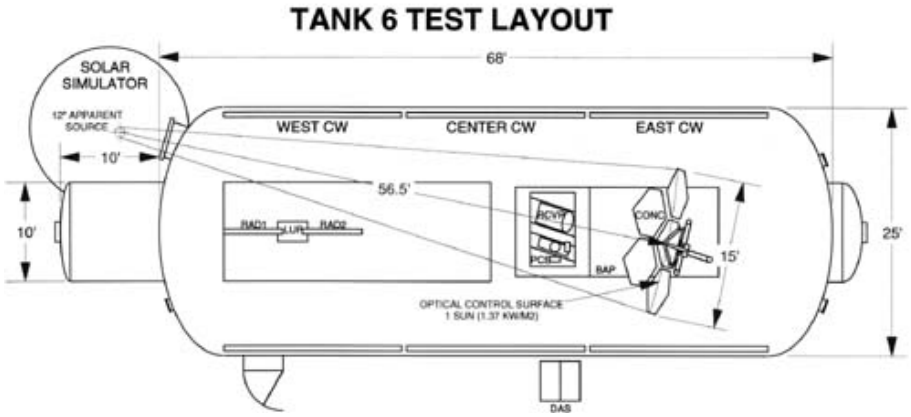

Figure 5(a).—Top view schematic of Tank 6, showing solar simulator and primary concentrator.

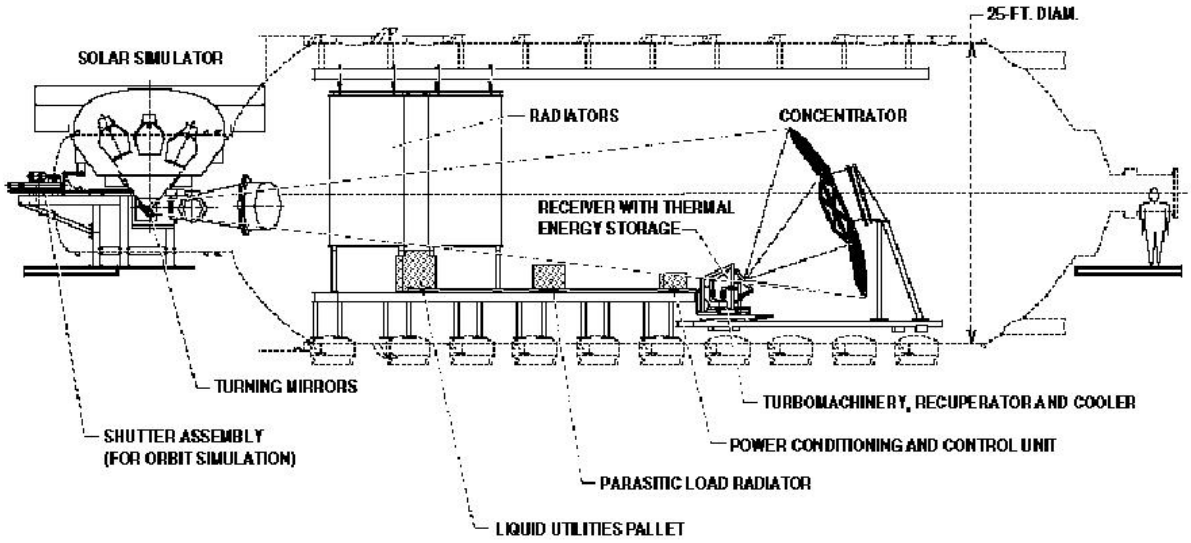

Figure 5(b).—Side view schematic of Tank 6 showing, location of receiver, which was the RSC in this case.

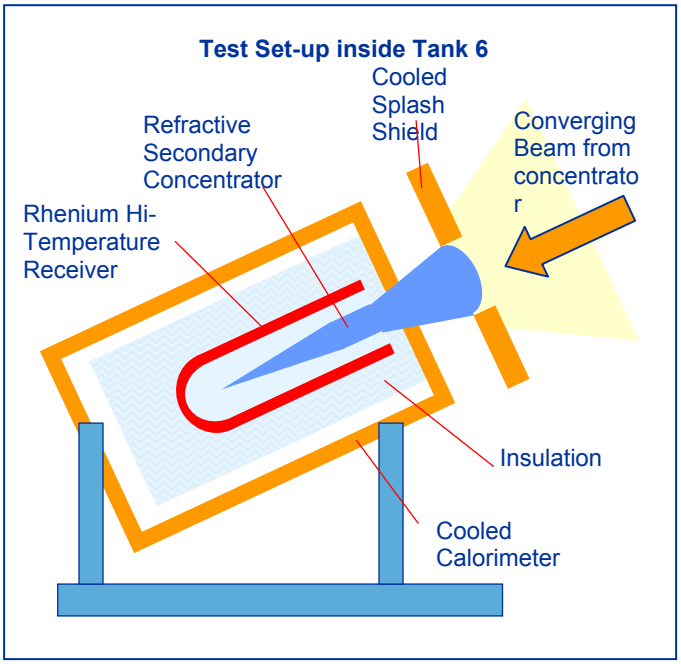

Figure 5(c).—Set-up for RSC test in Tank 6.

We briefly summarize the three tests. It should be noted that the temperatures were measured with thermocouples in the test setup and are only approximate. The actual temperature of the crystal was very hard to determine. Further, the different configurations of the tests meant the thermocouples were at different locations and hence not directly comparable.

(1) April 17, 2000. These were efficiency tests, run at low temperature and high power. A rhenium receiver was not used and the output of secondary was directed into a calorimeter. The tests are described in detail in reference 5.

(2) August 30, 2001. In this case the crystal was held in place with eight spring loaded shoes, to allow for expansion, as shown in figure 6. Two tests were run with the rigid concentrator—one at lower temperatures without the Re receiver and one at higher temperatures with the Re receiver. The high temperature test had an approximate maximum receiver temperature of (1300 °C) 2371 °F and an approximate maximum cone temperature of (582 °C) 1080 °F. The crystal cracked and failed in these tests. These tests are described in detail in reference 6.

(3) March 31, 2004. In this case a new holder was designed for minimal contact stress. A machineable ceramic insulation was fabricated to fit in a glove-like fashion around the RSC with a Mo sheet in between, as shown in figure 7. In 2004 two tests were run—one test with an inflatable concentrator at a lower temperature and one at mid-temperature with the rigid concentrator and Re receiver. For the mid-temperature exposure the maximum receiver temperature was approximately (649 °C) 1200 °F and the maximum cone temperature was approximately (438 °C) 820 °F. Again the crystal failed.

Although the sapphire crystal failed in the second and third tests, a good deal can be learned from a post-analysis of the failed RSC. The tests exhibit some similarities and some differences. Both failed crystals exhibited similar features, including internal discoloration in the conical region and a clear brittle failure origin. The crystal from the 2004 mid-temperature test exhibited a metallic deposit on the extractor.

Materials from both the tank tests and laboratory coupon tests were examined with optical microscopy and scanning electron microscopy (SEM) with energy dispersive spectroscopy (EDS) for elemental analyses. A portion of the post tank test crystal was also analyzed with Secondary Ion Mass Spectrometry (SIMS) by Evans Analytical Labs of East Windsor, New Jersey.

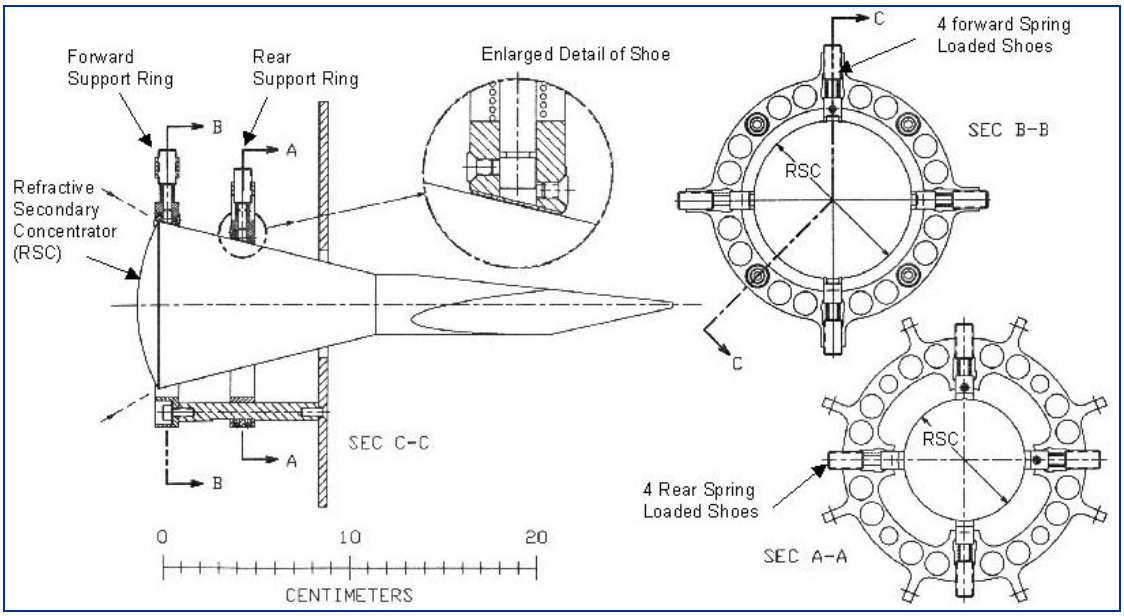

Figure 6.—Schematic of the mounting arrangement used in the first test.

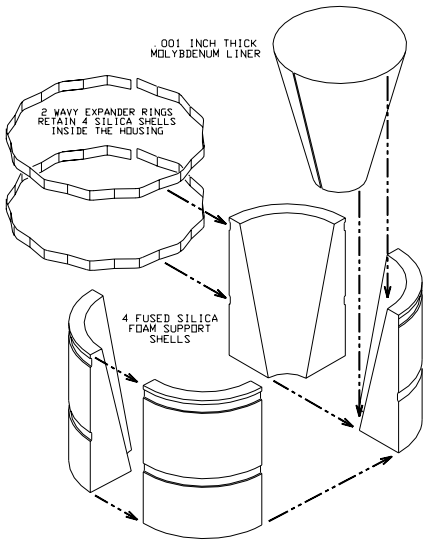

Figure 7.—Schematic of the mounting arrangement used in the second test.

3. Materials Issues With the Ceramic Crystal

Many factors determine the operating temperature range of the ceramic crystal. These factors are in regard to thermochemical, physical/optical, and thermomechanical stability. In regard to thermochemical stability the major issues are vaporization, phase transformations, and interfacial stability. An analysis of these allows us to set a thermochemical temperature limit for sapphire and fused silica.

3.1 Vaporization of the Oxide

The most obvious chemical issue is simple vaporization of the oxide at high temperatures. Vaporization leads to simple material loss, possible roughening of the surface, and deposition of the crystal composition on colder parts of the system. The first issue is to establish an acceptable vapor pressure. In a vacuum, vapor pressure (P) is related to flux (J) by the Hertz-Knudsen-Langmuir equation:

$$J\left(\frac{mole}{cm^2 \sec}\right) = \frac{P}{\sqrt{2\pi MRT}} = 44.33\frac{P(atm)}{\sqrt{M(gm/mol)T(K)}} \tag{1}$$

Here M is the molecular weight, R is the gas constant, and T is the absolute temperature.

We can derive an acceptable vapor pressure by relating this to recession or material loss rate. As will be shown, the vapor species above Al_2O_3(s) consist of a mix of Al(g), AlO(g), AlO_2(g), Al_2O(g), and other species depending on conditions. The vapor species above SiO_2(s) consist of a mixture of SiO(g), SiO_2(g), and other species depending on conditions. For this approximation, it is reasonable to take the average molecular weight of the vapor from MO(g) (where M is Si or Al), which is 44 or 45 gm/mole. For this estimation, we take the average 44.5 gm/mole. Similarly we take the average density for fused silica (2.19 gm/cc) and sapphire (3.965 gm/cc) of 3.1 gm/cc. We take an average application temperature of 1500 K. So our recession rate $(\widetilde{R})$ estimate becomes:

$$J\left(\frac{gm}{cm^2 hr}\right) = 44.33\frac{P(atm)}{\sqrt{M(gm/mol)T(K)}}M(gm/mol)\frac{3600\sec}{1hr} =$$

$$1.596\cdot 10^5\, P(atm)\sqrt{\frac{M(gm/mol)}{T(K)}}$$

$$M = 44.5$$

$$J\left(\frac{gm}{cm^2 hr}\right) = 1.596\cdot 10^5\, P(atm)\sqrt{\frac{44.5}{T(K)}} = 1.1\cdot 10^5\frac{P}{\sqrt{T}}$$

$$\widetilde{R}\left(\frac{cm}{hr}\right) = J\left(\frac{gm}{cm^2 hr}\right)\frac{1}{\rho}\left(\frac{cm^3}{gm}\right) = 3.5\cdot 10^5\frac{P}{\sqrt{T}}$$

$$T = 1500$$

$$\widetilde{R}\left(\frac{cm}{hr}\right) = 9000P(atm) \qquad (2)$$

Table 1 lists a range of vapor pressures and corresponding recession rates at 1500 K.

TABLE 1.—VAPOR PRESSURES AND RESULTING APPROXIMATE RECESSION RATES

Vapor pressure, (atm)	Recession rate, (cm/hr)	Recession after 1000 hr, (cm)
1×10^{-4}	9×10^{-1}	900
1×10^{-5}	9×10^{-2}	90
1×10^{-6}	9×10^{-3}	9
1×10^{-7}	9×10^{-4}	0.9
1×10^{-8}	9×10^{-5}	0.09
1×10^{-9}	9×10^{-6}	0.009
1×10^{-10}	9×10^{-7}	0.0009

The acceptable recession rate depends on the expected life. Let us take 1000 hr at temperature, which gives the quantities listed in the column at the right. On basis of this a vapor pressure of 10^{-9} to 10^{-10} atm is acceptable.

Figures 8 and 9 are the calculated pressures of vapor species above Al_2O_3 and SiO_2, respectively. These show the pressures of each individual species as well as the total vapor pressure. The computation was done with a fixed volume of 1 liter. Changing this volume did not significantly affect the results, unless the volume became extremely large.

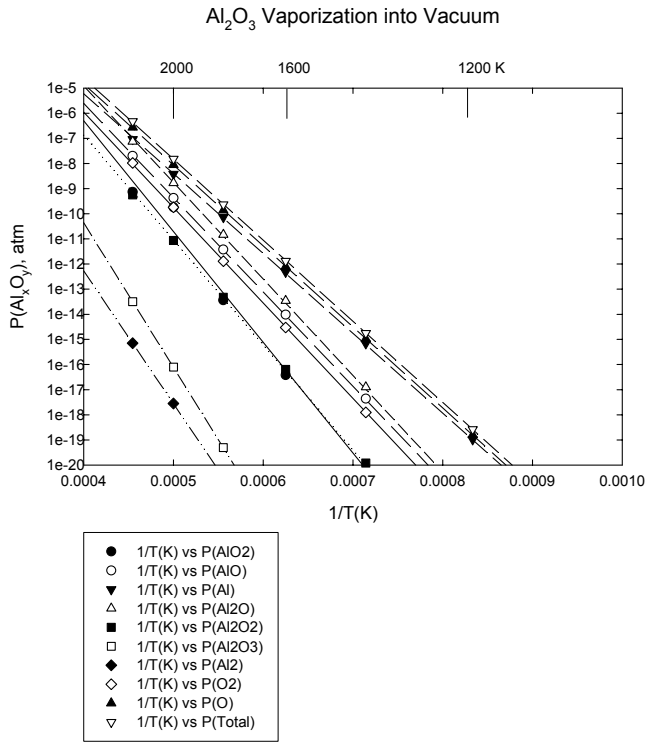

Figure 8(a).—Vapor pressures of the gas phase species over Al_2O_3 in a vacuum.

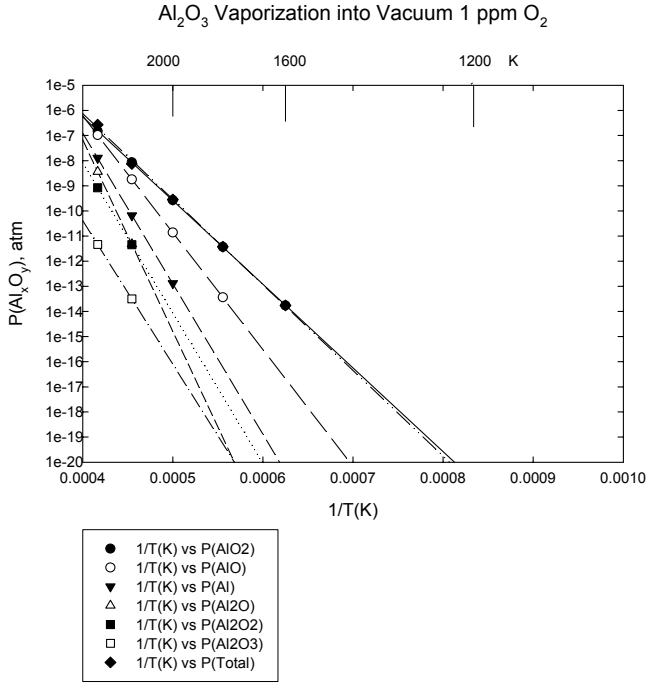

Figure 8(b).—Vapor pressures of the gas phase species over Al_2O_3 with 1 ppm O_2.

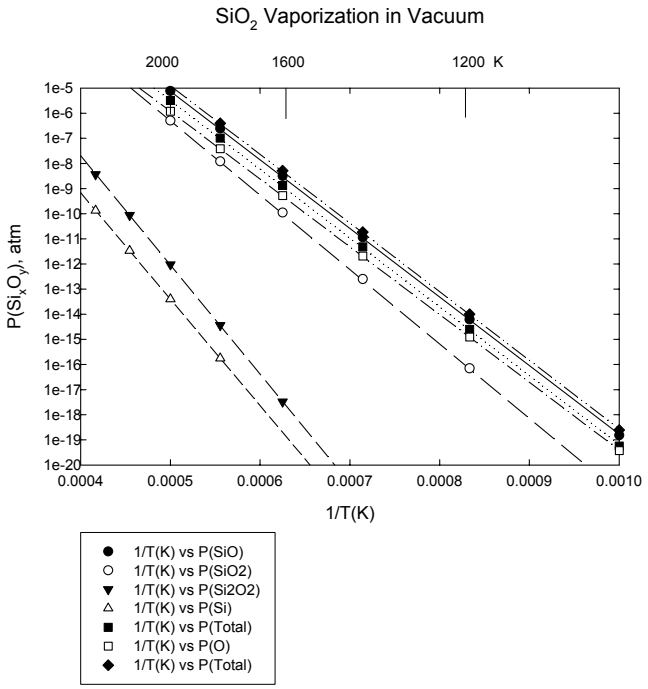

Figure 9(a).—Vapor pressures of the gas phase species over SiO_2 in a vacuum.

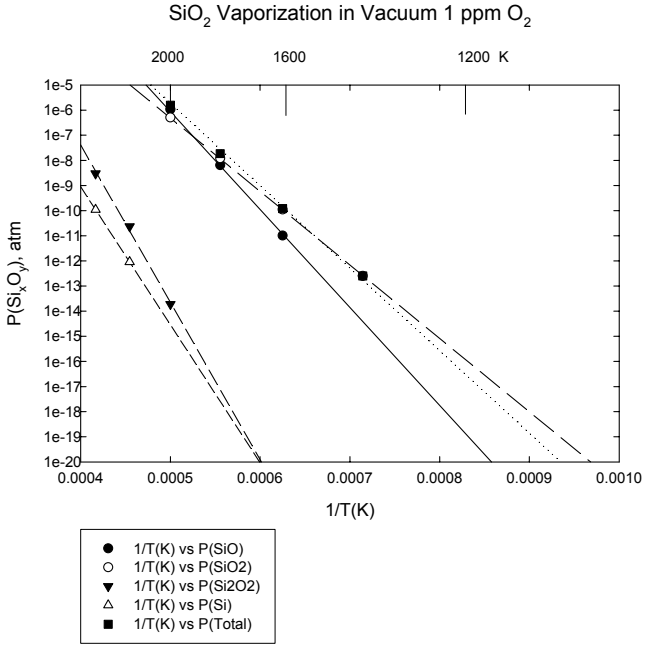

Figure 9(b).—Vapor pressures of the gas phase species over SiO_2 with 1 ppm O_2.

Two calculations were done for both Al_2O_3 and SiO_2—one for vaporization into a high vacuum and one for vaporization into an overpressure of oxygen of 10^{-6} bar (1 ppm). This amount of oxygen can be reasonably expected in the soft vacuum of space and in a real system. In the case of oxide vaporization, an overpressure of oxygen will suppress reactions which decompose to an oxygen product such as:

$$SiO_2(s) = SiO(g)+½\ O_2(g) \quad (3)$$

This is evident by comparing figure 8(a) and (b) and comparing figure 9(a) to (b). In both cases, the overpressure of 10^{-6} bar oxygen suppresses the total vapor pressure of the crystal by about one order of magnitude.

If we take 10^{-10} bar to be conservative, in vacuum Al_2O_3 is acceptable to ~1800 K and SiO_2 is acceptable to ~1500 K. In 1 ppm O_2, these upper limits increase about 100 K. Before these temperatures are reached, other issues will limit the usefulness of the crystal. These will be discussed in subsequent sections.

3.2 Preservation of Optical Properties at High Temperatures

Clearly, the optical properties of the crystal are central to this concept. These include transmission and refractive index. Figure 10 is a photograph of the failed sapphire crystal after the test on March 31, 2004. Note that the conical portion of the crystal shows a rose/brown color, whereas the extractor shows a darker color. Clearly these color changes lead to significant changes in the optical properties. Note also that the center between the conical region and the extractor is clear.

Closer examination of the extractor indicated that it was coated with a thin outer metallic film. An image and an EDS analysis of this deposit are shown in figure 11(a) and (b). Clearly Re was transported from the receiver cavity to the extractor. In a high vacuum the vapor pressure of Re is very low and it is unlikely that sufficient Re(g) would be transported to form the observed film. However, as will be discussed in the next session, a small amount of oxygen creates stable vapor phase rhenium oxides, such as $Re_2O_7(g)$. These may form on the receiver walls, transport to the cooler extractor, and decompose on the extractor to form the metal film.

Photomicrographs, such as in figure 11(a), indicate the film is ~10 nm. The receiver was hottest about 0.16 hr. From this information we estimate the vapor flux of $Re_2O_7(g)$ impinging on the extractor to be $\sim 1.91\times10^{-10}$ mole/cm^2-sec. Using the FactSage Code (10), we calculate vapor pressures above ReO_2/Re from 400 to 1000 K. The in turn are converted to fluxes and the fluxes are compared to the above value. We thus estimate a maximum temperature for the extractor of ~890 K = 617 °C = 1,142 °F. This is consistent with the measured temperatures for the third test as described previously.

Figure 10.—Photograph of crystal after 2004 mid-temperature test.

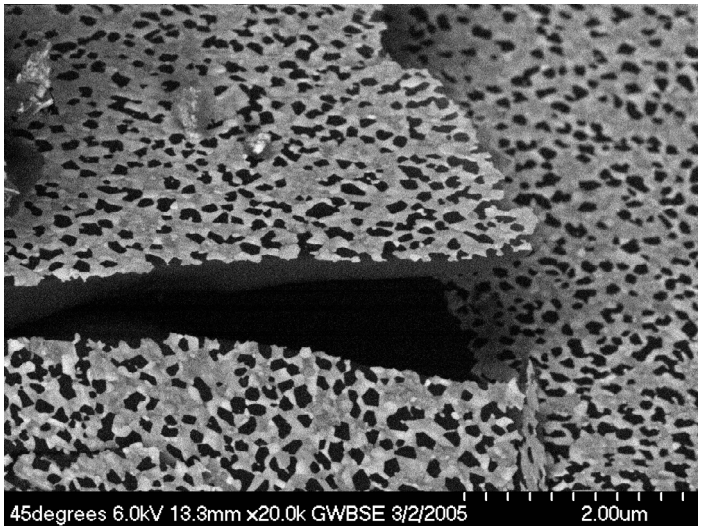

Figure 11(a).—Backscattered electron image of deposited film on extractor.

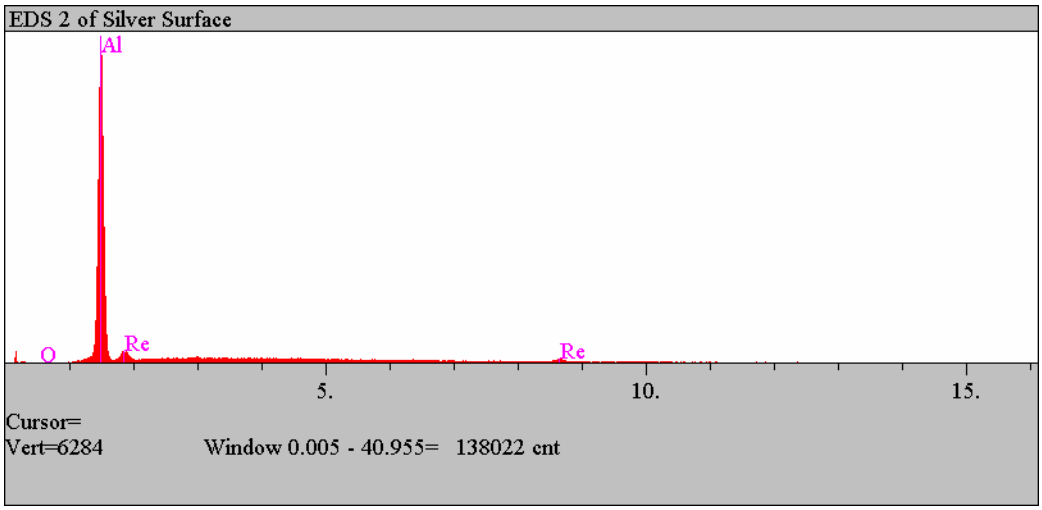

Figure 11(b).—EDS spectra of deposited film.

As noted the conical portion of the crystal has a rose-colored appearance. This phenomena is well-documented for sapphire crystals exposed to ultra-violet (UV) radiation (refs. 11 to 13) and termed "solarization". The general principles of solarization are understood; the details are not. Figure 12 is a spectrum for a portion of two sapphire as-fabricated crystals (ref. 13). Note the absorption peaks at 205, 255, and 395 nm. The large absorption at 205 nm in the UV is the usual indicator of susceptibility to solarization. This is due to UV is absorbed by an oxygen vacancy with two electrons (f center). Most of this energy goes into generating phonons. However some may also eject electrons from the oxygen vacancy creating vacancies with one electron (f^+ centers) and vacancies with three electrons (f^- centers). These in turn may lead to absorptions in the visible region. A very low concentration of color centers will create a color change.

The details of oxygen vacancy formation are not well-understood. It is likely that some combination of trace impurities and processing conditions create vacancies. Some investigators have suggested that Ti^{+4} impurities may be a cause of vacancy formation. However other impurities such as Cr, Fe, and Mg may also play a role as well as the oxygen potential in processing.

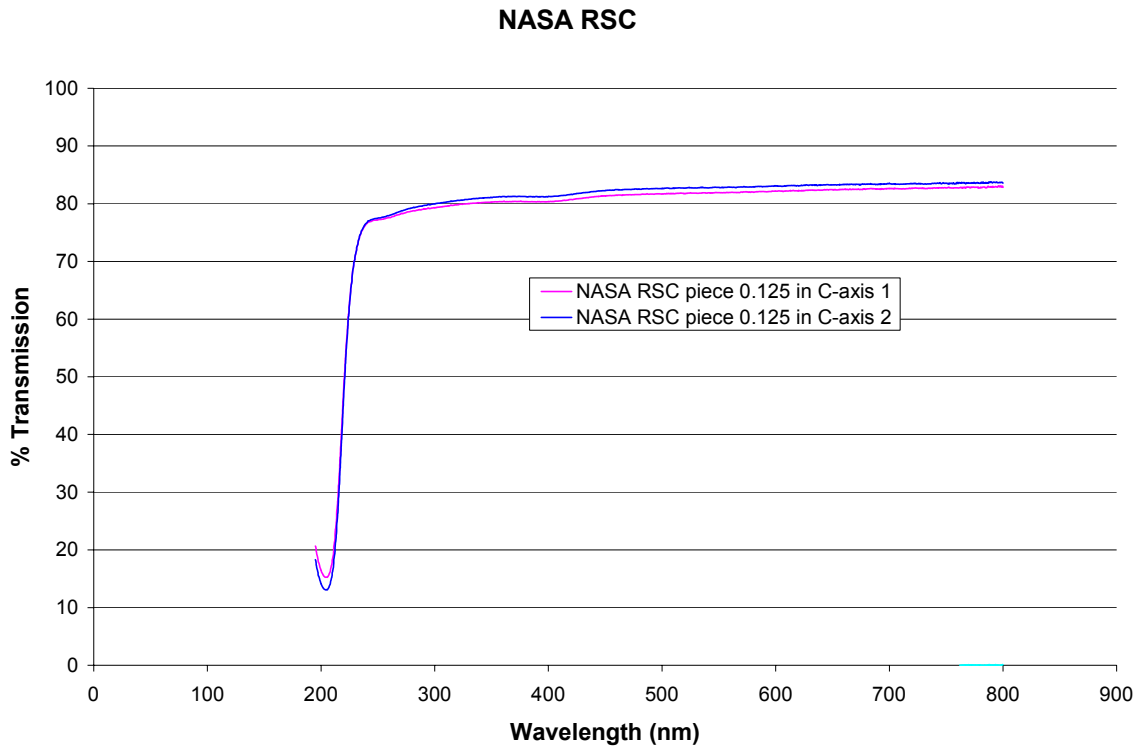

Figure 12.—Absorption spectra taken by Crystal Systems, Inc. of the sapphire samples (ref. 11).

While most of the evidence suggests solarization of the sapphire, there are some data that do not support solarization. First is the extent of UV exposure. Referring to figure 3, we see that the xenon lamp spectra drops off very dramatically in the UV region. The amount of power in the UV region is probably only ~1 percent of the total. However the xenon lamps direct a lot of power on the crystal, so this amount of UV may or may not be sufficient to induce solarization. Second, a mild heat treatment should neutralize the charged oxygen vacancies and remove the color. This is termed 'UV hardening.' The actual test conditions involve heating and should, in theory, neutralize the charged vacancies. This may have been the reason that the central portion of the crystal remain clear. Clearly more research is necessary to understand and mitigate the solarization issue with sapphire. Other candidate materials, such as silica, need to be thoroughly pre-tested for solarization.

A SIMS analysis of samples from the sapphire crystal after the March 2004 test is given in figure 13(a) and (b). Note there is relatively little difference between the as-received crystal and the crystal which had solarized. The impurities (in approximate order of concentration) include Si, Ti, Cu, Na, K, Ca, Fe, Mg, and Cr. Microprobe analysis of a polished section of the sample showed only a weak Si signal and the content of Si was about 0.08 mass percent or 80 ppm. It is unlikely that the Si leads to the color change; but the other elements may play a role.

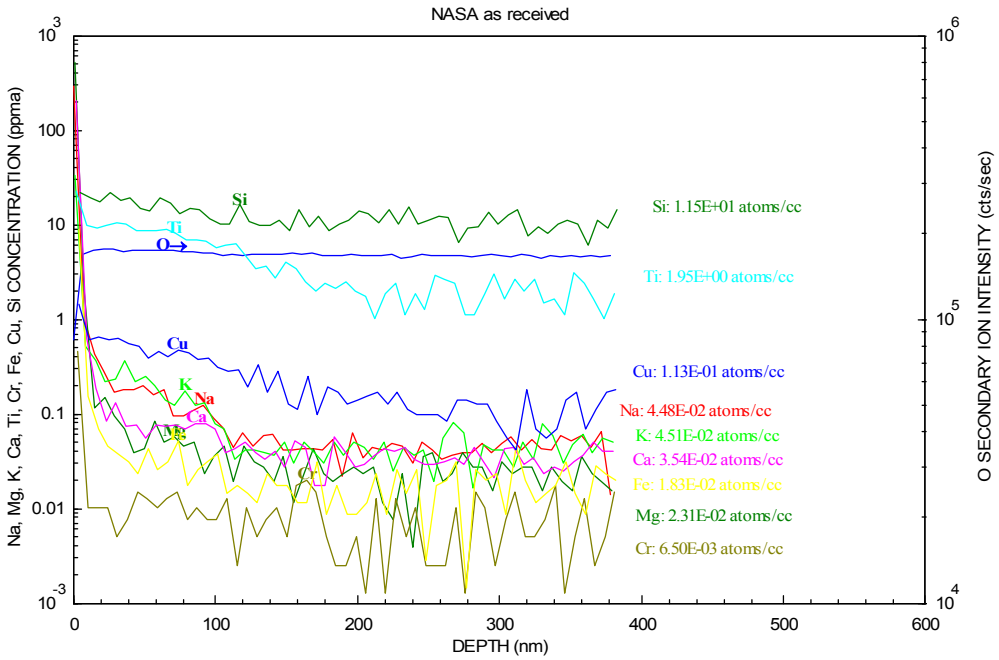

Figure 13(a).—SIMS results from as-received sapphire, before exposure.

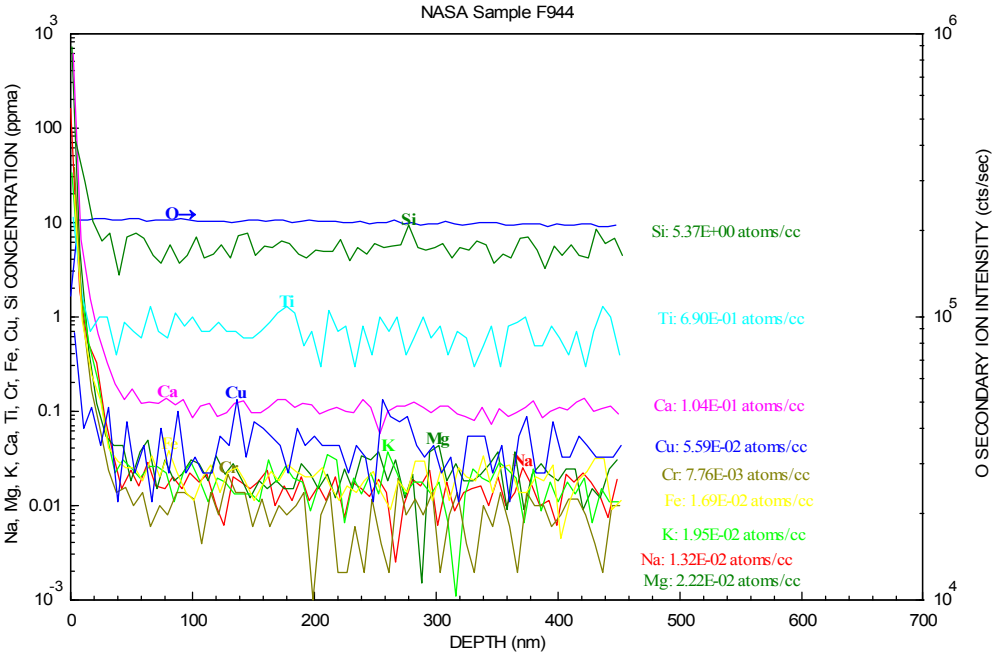

Figure 13(b).—SIMS results from section cut from the RSC used in the March 21, 2004 test.

3.3 Mechanical Properties of the Crystal

Thermomechanical stability of the crystal is the key issue in the operation of this system and this issue has been treated in other reports (refs. 2 and 14). The main issues will be briefly summarized here since mechanical and chemical issues in this complex system are closely related.

Since the crystal will necessarily go through heating/cooling cycles, thermal shock is a major issue. Oxide ceramics tend to be quite susceptible to thermal shock. A temperature distribution throughout the crystal leads to differences in thermal expansion and thus tensile stresses within the crystal. Temperature distributions and stress distributions were calculated for the crystal before the tests and indicated the stresses were below the fracture stress of alumina (ref. 15). However machining flaws on the surface or fabrication flaws within the crystal itself can be stress concentrators (see fig. 14). Further the crystal may have darkened during the test and did not transmit light properly, so there were likely larger than predicted temperature excursions.

Vitreous or fused (non-crystalline) silica has a zero coefficient of thermal expansion and therefore shows extremely good thermal shock behavior. At this point in the development of a solar thermal secondary refractor, vitreous silica is the most promising material. As noted, current studies of this concept for terrestrial applications utilize silica (refs. 7 to 9). Care must be taken with vitreous silica to limit the temperature below the temperature of devitrification (crystallization) which is ~1200 °C. In addition to temperature, impurities such as metal cations also induce devitrification and the system must be kept clear of these.

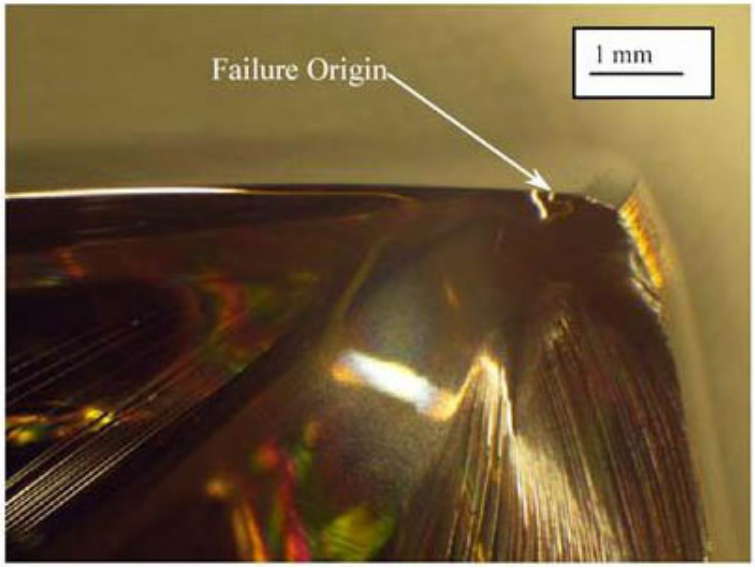

Figure 14.—View of fracture surface (J. Salem, NASA Glenn)
on sapphire crystal tested on March 31, 2004.
Note fracture origin near surface (ref. 2).

4. Stability of High-Temperature Metals

As shown in figure 1, the proposed system will contain some metals. These are the refractory metals—niobium (Nb), tantalum (Ta), molybdenum (Mo), tungsten (W), and rhenium (Re). These are high melting and stable in very low-oxygen environments. The densities and melting points for these metals are listed in table 2 (ref. 16). We limit our discussion here to the pure metals; however there are refractory alloys that show improved mechanical and chemical properties at high temperatures. In many high temperature systems, carbon is also used and we include a discussion of carbon interactions as well.

TABLE 2.—DENSITIES AND MELTING POINTS OF REFRACTORY METALS (REF. 16)

Refractory metal	Density, (gm/cc)	Melting point, °C (°F)
Niobium (Nb)	8.57	2468 (4474)
Tantalum (Ta)	16.6	2996 (5425)
Tungsten (W)	10.22	2610 (4730)
Molybdenum (Mo)	19.25	3410 (6170)
Rhenium (Re)	21.04	3180 (5755)

The problem with most of these metals is their high reactivity with even trace amounts of oxygen. For example, rhenium is quite readily attacked by 334 ppm of oxygen in argon at temperatures as low as 600 °C (ref. 17). Although a small amount of oxygen may suppress the vaporization of the oxide crystal, a small amount of oxygen may lead to degradation of the refractory metal parts. Since these trace amounts of oxygen are always present, it is important to understand and assess the effect of oxygen on these refractory metals.

Each of these metals behaves differently at different temperatures in the presence of oxygen. Some form condensed phase oxides, some form highly volatile oxides, and some form a mixture of both. We assess the behavior of these metals in oxygen with a consistent, thermodynamically sound approach. As discussed, we use the FactSage Thermochemical Software (ref. 10). The results of the calculations are presented in table 3 at 1000, 1500, and 2000 K. Where possible, calculations were done for two oxygen pressures.

First we calculate the oxygen pressure set by the metal/metal oxide equilibrium. This is the most metal-rich oxide. The refractory oxides all form condensed phase oxides, which are not protective. So it is reasonable to assume a small amount of oxide forms and is in equilibrium with the metal. The resultant pressures of the various vapor species are listed in table 3. For practical purposes only the species with the highest vapor pressures need to be considered.

Note that Nb and Ta have only a few vapor species with relatively low vapor pressures and therefore look acceptable. However, as noted, the solid oxides of Ta and Nb are non-protective and the oxidation rates are very high (ref. 18).

The other refractory metals—Mo, W, and Re—form many complex gaseous metal oxides, as indicated in table 3. Note that in some cases the dimeric and trimeric species have a higher vapor pressure than the monomeric species. Re is unique in that it forms a stable condensed phase oxide at 1000 K, but not at the higher temperatures. At these higher temperatures we cannot do the calculation for a stable metal/metal-oxide equilibrium.

The first set of calculations describes the situation where the oxygen pressure can be held to a very low value set by the metal/metal-oxide equilibrium (M/MO_x). In some applications the oxygen pressure may be higher due to the soft vacuum of space or general out-gassing of other components in a system.

The second set of calculation fixes the oxygen at 1 ppm, or 1×10^{-6} atm. This is done using the "target" feature in the equilibrium module in FactSage (ref. 10). Metal and oxygen reactants were used with the condition that the output pressure of oxygen be 1×10^{-6} atm. The results of these calculations are also shown in table 3.

In an atmosphere of 1×10^{-6} atm O_2, all of the refractory metals will form a condensed phase oxide at high temperatures (except Re) as the stable phase. Since this is non-protective and the calculation assumes an infinite amount of oxygen to give a constant pressure of 1×10^{-6} atm of O_2, the metal is entirely consumed to form oxide. In practice there may be some kinetic limitations (e.g., gas phase diffusion or limited protection from the oxide) which preclude this from happening. But nonetheless, this calculation gives some basis for comparing the metals.

The results for the 1 ppm oxygen case are summarized in figure 15. Again, Nb and Ta appear to be acceptable. But the extent of solid oxide formation must be considered. Note that 1 ppm oxygen generates a large vapor pressure of Re_2O_7, even at temperatures as low as 500 K. This is consistent with oxidation studies (ref. 17). As noted, Re is stable as a bare metal at higher temperatures. Interestingly the stability of some of the gaseous oxides appears to decrease with temperature.

In summary, it is difficult to definitively assess the behavior of refractory metals in low-oxygen environments. The major issues are rapidly growing oxides and high vapor pressures of gaseous metal oxides. A detailed analysis shows:

(1) Lower $P(O_2)$ gives lower metal oxide vapor pressure.

(2) While Nb and Ta have low metal oxide vapor pressures, the rapidly growing condensed oxide must be considered.

(3) The benefits of Re are that it is stable as the metal at the highest temperatures. However trace amounts of oxygen (e.g., ~ ppm) will lead still lead to volatile metal oxides.

As noted, carbon is often used as a construction material for high temperature, non-oxidizing systems. At high temperatures carbon reacts readily with oxygen:

$$C(s)+½\ O_2(g) = CO(g) \tag{4a}$$

$$C(s)+O_2(g) = CO_2(g) \tag{4b}$$

Unless the oxygen pressure is extremely low (i.e., $< \sim10^{-10}$ atm), some carbon will be lost via these reactions. So it is best to avoid the use of carbon or graphite containing materials.

TABLE 3.—THERMODYNAMIC ANALYSES OF REFRACTORY METAL OXIDATION

			Oxygen Pressure Set by M/MOx		$P(O_2)$ fixed at 1×10^{-6}	
Metal	Condensed phase oxide(s)	Temperature, K	M/MOx Pressure at Metal/Oxide Interface, (atm)	$P(O_2)$ set by M/MOx Vapor pressure of metal species, atm	Solid phase	Vapor pressures of metal species, atm
Nb	Nb_2O_5, NbO_2	1000	Nb/NbO $P(O) = 1.04\times10^{-27}$ $P(O_2) = 4.44\times10^{-35}$	$P(NbO_2) = 3.14\times10^{-23}$ $P(NbO) = 2.84\times10^{-23}$ $P(Nb) = 1.38\times10^{-30}$	Nb_2O_5	$P(NbO_2) = 1.42\times10^{-25}$ $P(NbO) = 8.58\times10^{-40}$
		1500	Nb/NbO $P(O) = 4.51\times10^{-16}$ $P(O_2) = 1.25\times10^{-20}$	$P(NbO_2) = 2.24\times10^{-12}$ $P(NbO) = 1.00\times10^{-12}$ $P(Nb) = 5.44\times10^{-18}$	Nb_2O_5	$P(NbO_2) = 7.42\times10^{-13}$ $P(NbO) = 3.72\times10^{-20}$ $P(Nb) = 2.26\times10^{-32}$
		2000	Nb/NbO $P(O) = 2.83\times10^{-10}$ $P(O_2) = 1.81\times10^{-13}$	$P(NbO_2) = 4.65\times10^{-7}$ $P(NbO) = 1.55\times10^{-7}$ $P(Nb) = 1.81\times10^{-13}$	Nb_2O_5	$P(NbO_2) = 8.84\times10^{-7}$ $P(NbO) = 1.26\times10^{-10}$ $P(Nb) = 3.50\times10^{-18}$
Ta	Ta_2O_5	1000	Ta/Ta_2O_5 $P(O) = 2.41\times10^{-27}$ $P(O_2) = 2.38\times10^{-34}$	$P(TaO_2) = 6.57\times10^{-24}$ $P(TaO) = 2.30\times10^{-25}$ $P(Ta) = 3.36\times10^{-34}$	Ta_2O_5	$P(TaO_2) = 8.16\times10^{-31}$
		1500	Ta/Ta_2O_5 $P(O) = 6.96\times10^{-16}$ $P(O_2) = 2.98\times10^{-20}$	$P(TaO_2) = 5.93\times10^{-13}$ $P(TaO) = 3.19\times10^{-14}$ $P(Ta) = 1.31\times10^{-20}$	Ta_2O_5	$P(TaO_2) = 2.46\times10^{-16}$ $P(TaO) = 2.28\times10^{-24}$ $P(Ta) = 1.63\times10^{-37}$
		2000	Ta/Ta_2O_5 $P(O) = 3.40\times10^{-10}$ $P(O_2) = 2.62\times10^{-13}$	$P(TaO_2) = 1.31\times10^{-7}$ $P(TaO) = 9.73\times10^{-9}$ $P(Ta) = 8.36\times10^{-14}$	Ta_2O_5	$P(TaO_2) = 2.96\times10^{-9}$ $P(TaO) = 1.13\times10^{-13}$ $P(Ta) = 4.96\times10^{-22}$
Mo	MoO_3, MoO_2	1000	Mo/MoO_2 $P(O) = 3.52\times10^{-21}$ $P(O_2) = 5.08\times10^{-22}$	$P(MoO_3) = 7.81\times10^{-17}$ $P(Mo_2O_6) = 2.97\times10^{-19}$ $P(MoO_2) = 2.49\times10^{-19}$ $P(Mo_3O_9) = 8.95\times10^{-23}$ $P(MoO) = 3.15\times10^{-24}$	MoO_3	$P(Mo_4O_{12}) = 3.46\times10^{-4}$ $P(Mo_3O_9) = 2.93\times10^{-4}$ $P(Mo_5O_{15}) = 3.17\times10^{-5}$ $P(Mo_2O_6) = 6.56\times10^{-7}$ $P(MoO_3) = 1.16\times10^{-10}$

TABLE 3.—THERMODYNAMIC ANALYSES OF REFRACTORY METAL OXIDATION (Continued)

			Oxygen Pressure Set by M/MOx			$P(O_2)$ fixed at 1×10^{-6}
Metal	Condensed phase oxide(s)	Temperature, K	M/MOx Pressure at Metal/Oxide Interface, (atm)	$P(O_2)$ set by M/MOx Vapor pressure of metal species, atm	Solid phase	Vapor pressures of metal species, atm
		1500	Mo/MoO_2 $P(O) = 9.26\times10^{-12}$ $P(O_2) = 5.28\times10^{-12}$	$P(MoO_3) = 3.52\times10^{-8}$ $P(Mo_2O_6) = 4.97\times10^{-9}$ $P(MoO_2) = 1.04\times10^{-9}$ $P(Mo_3O_9) = 2.10\times10^{-10}$ $P(MoO) = 4.09\times10^{-13}$ $P(Mo_4O_{12}) = 7.68\times10^{-14}$ $P(Mo) = 7.54\times10^{-16}$ $P(Mo_5O_{15}) = 4.76\times10^{-18}$	MoO_2	$P(Mo_3O_9) = 1.73\times10^{-2}$ $P(Mo_4O_{12}) = 2.75\times10^{-3}$ $P(Mo_2O_6) = 9.40\times10^{-4}$ $P(Mo_5O_{15}) = 7.42\times10^{-5}$ $P(MoO_3) = 1.53\times10^{-5}$ $P(MoO_2) = 1.04\times10^{-9}$ $P(MoO) = 9.40\times10^{-16}$
		2000	Mo/MoO $P(O) = 4.28\times10^{-7}$ $P(O_2) = 4.15\times10^{-7}$	$P(MoO_3) = 4.80\times10^{-4}$ $P(Mo_2O_6) = 3.15\times10^{-4}$ $P(Mo_3O_9) = 1.20\times10^{-4}$ $P(MoO_2) = 4.61\times10^{-5}$ $P(Mo_4O_{12}) = 1.14\times10^{-7}$ $P(Mo_5O_{15}) = 1.08\times10^{-9}$	MoO_2	$P(Mo_2O_6) = 7.58\times10^{-4}$ $P(MoO_3) = 7.45\times10^{-4}$ $P(Mo_3O_9) = 4.50\times10^{-4}$ $P(MoO_2) = 4.61\times10^{-5}$ $P(Mo_4O_{12}) = 4.17\times10^{-6}$ $P(MoO) = 7.36\times10^{-8}$ $P(Mo_5O_{15}) = 9.69\times10^{-9}$ $P(Mo) = 1.33\times10^{-10}$ $P(Mo_2) = 2.96\times10^{-16}$
W	WO_2, WO_3, W_7O_{19}, $W_{10}O_{29}$	1000	W/WO_2 $P(O) = 3.56\times10^{-21}$ $P(O_2) = 5.20\times10^{-22}$	$P(W_3O_9) = 7.25\times10^{-17}$ $P(W_2O_6) = 5.60\times10^{-17}$ $P(W_3O_8) = 6.19\times10^{-18}$ $P(W_4O_{12}) = 5.48\times10^{-20}$ $P(WO_3) = 3.17\times10^{-20}$ $P(WO_2) = 1.05\times10^{-23}$ $P(W_5O_{15}) = 4.48\times10^{-25}$ $P(WO) = 5.22\times10^{-28}$	WO_3	$P(W_3O_9) = 1.80\times10^{-12}$ $P(W_2O_6) = 1.56\times10^{-13}$ $P(W_4O_{12}) = 3.96\times10^{-14}$ $P(W_5O_{15}) = 9.42\times10^{-18}$ $P(WO_3) = 9.23\times10^{-19}$

TABLE 3.—THERMODYNAMIC ANALYSES OF REFRACTORY METAL OXIDATION (Continued)

			Oxygen Pressure Set by M/MOx			$P(O_2)$ fixed at 1×10^{-6}
Metal	Condensed phase oxide(s)	Temperature, K	M/MOx Pressure at Metal/Oxide Interface, (atm)	$P(O_2)$ set by M/MOx Vapor pressure of metal species, atm	Solid phase	Vapor pressures of metal species, atm
		1500	W/WO_2 $P(O) = 9.75\times10^{-12}$ $P(O_2) = 5.85\times10^{-12}$	$P(W_3O_9) = 2.77\times10^{-6}$ $P(W_2O_6) = 9.97\times10^{-7}$ $P(W_3O_8) = 5.07\times10^{-7}$ $P(W_4O_{12}) = 1.30\times10^{-7}$ $P(WO_3) = 2.92\times10^{-10}$ $P(WO_2) = 1.98\times10^{-12}$ $P(WO) = 1.03\times10^{-15}$ $P(W) = 7.70\times10^{-23}$	WO_3	$P(W_3O_9) = 2.05\times10^{-4}$ $P(W_4O_{12}) = 4.07\times10^{-5}$ $P(W_2O_6) = 1.76\times10^{-5}$ $P(W_5O_{15}) = 1.62\times10^{-7}$ $P(W_3O_8) = 9.10\times10^{-8}$ $P(WO_3) = 1.23\times10^{-9}$ $P(WO_2) = 2.02\times10^{-14}$ $P(WO) = 2.53\times10^{-20}$
		2000	$W/WO_{2.72}$ $P(O) = 3.88\times10^{-7}$ $P(O_2) = 3.41\times10^{-7}$	$P(W_3O_9) = 4.82\times10^{-2}$ $P(W_2O_6) = 2.53\times10^{-2}$ $P(W_3O_8) = 1.64\times10^{-2}$ $P(W_4O_{12}) = 8.53\times10^{-3}$ $P(W_5O_{15}) = 3.93\times10^{-5}$ $P(WO_3) = 1.12\times10^{-5}$ $P(WO_2) = 4.35\times10^{-7}$ $P(WO) = 9.63\times10^{-10}$ $P(W) = 2.49\times10^{-15}$	$WO_{2.72}$	$P(W_3O_9) = 3.76\times10^{-1}$ $P(W_4O_{12}) = 1.32\times10^{-1}$ $P(W_2O_6) = 9.95\times10^{-2}$ $P(W_3O_8) = 7.45\times10^{-2}$ $P(W_5O_{15}) = 1.20\times10^{-3}$ $P(WO_3) = 2.21\times10^{-5}$ $P(WO_2) = 5.03\times10^{-7}$ $P(WO_2) = 2.02\times10^{-14}$ $P(WO) = 6.51\times10^{-10}$ $P(W) = 9.84\times10^{-16}$
Re	ReO_2, ReO_3, Re_2O_7	500	Re/ReO_2 $P(O_2) = 7.65\times10^{-37}$	$P < 10^{-20}$	ReO_3	$P(Re_2O_7) = 1.26\times10^{-4}$
		1000	Re/ReO_2 $P(O_2) = 5.08\times10^{-14}$ $P(O) = 3.52\times10^{-17}$	$P(Re_2O_7) = 5.22\times10^{-7}$ $P(Re_2O_6) = 6.53\times10^{-8}$ $P(ReO_3) = 2.78\times10^{-9}$ $P(ReO_2) = 5.21\times10^{-17}$ $P(ReO) = 5.90\times10^{-23}$	ReO_3	$P(Re_2O_7) = 1.03\times10^{-1}$ $P(Re_2O_6) = 2.91\times10^{-6}$ $P(ReO_3) = 1.85\times10^{-8}$ $P(ReO_2) = 7.84\times10^{-20}$ $P(ReO) = 2.00\times10^{-29}$

TABLE 3.—THERMODYNAMIC ANALYSES OF REFRACTORY METAL OXIDATION (Concluded)

			Oxygen Pressure Set by M/MOx			$P(O_2)$ fixed at 1×10^{-6}
Metal	Condensed phase oxide(s)	Temperature, K	M/MOx Pressure at Metal/Oxide Interface, (atm)	$P(O_2)$ set by M/MOx Vapor pressure of metal species, atm	Solid phase	Vapor pressures of metal species, atm
		1500			Re	$P(Re_2O_7) = 4.04\times10^{-1}$ $P(Re_2O_6) = 3.85\times10^{-1}$ $P(ReO_3) = 3.03\times10^{-3}$ $P(ReO_2) = 3.93\times10^{-8}$ $P(ReO) = 1.54\times10^{-12}$
		2000			Re	$P(ReO_3) = 1.04\times10^{-5}$ $P(ReO_2) = 2.23\times10^{-7}$ $P(Re_2O_6) = 1.22\times10^{-8}$ $P(ReO) = 3.33\times10^{-9}$ $P(Re_2O_7) = 7.23\times10^{-11}$ $P(Re) = 2.42\times10^{-17}$

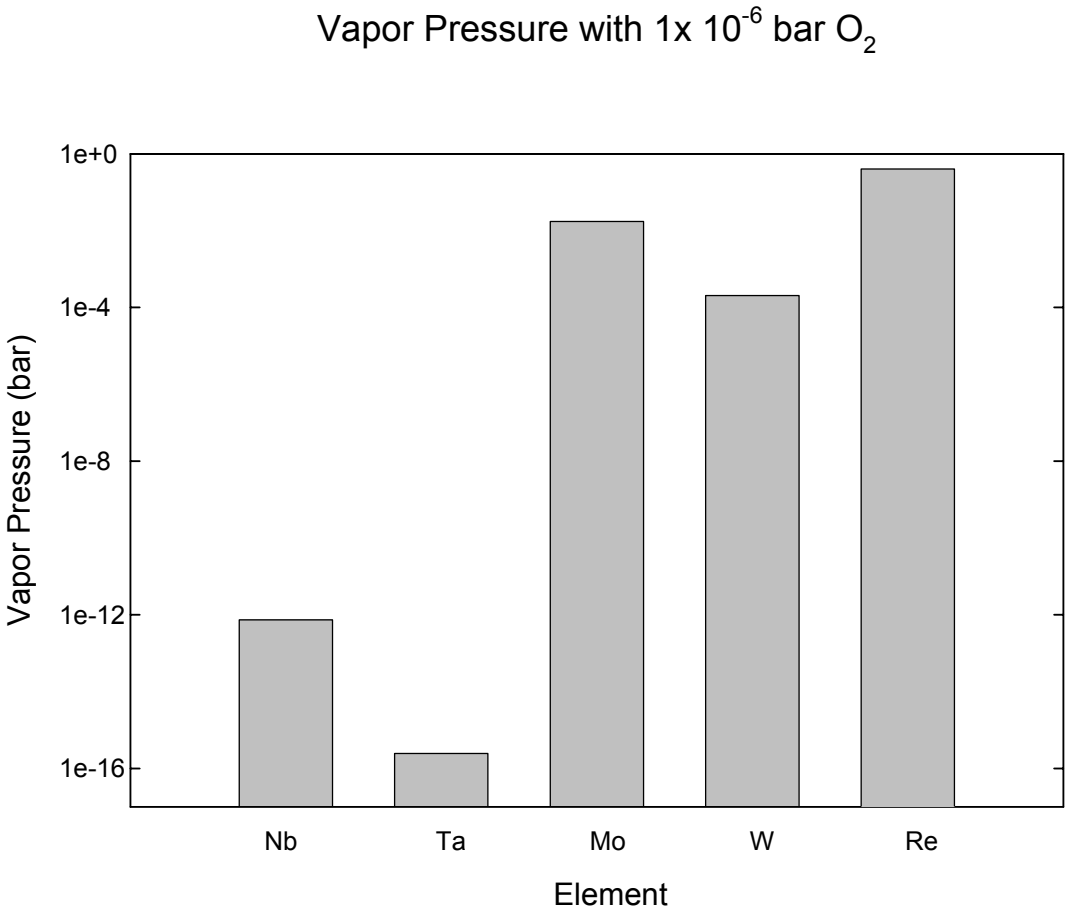

Figure 15.—Vapor pressures above refractory metals with a set $P(O_2)$ of 1×10^{-6} bar at 1500 K.

5. Interactions of Carbon and Refractory Metals With Al_2O_3 and SiO_2

5.1 Calculations

In the August 2001 test, the RSC was in contact with Ta. In the March 2004 test, the RSC was in contact with Mo. In this section we consider the possible high temperature reactions of the RSC with various refractory metals. Table 4 lists the possible combinations included in this study. Carbon is included for completeness and it will be shown that the oxides should not be in any contact with carbon. The compatibility of a metal and an oxide involves several considerations (ref. 19) including solid phase formation, gaseous phase formation, and oxygen solubility.

TABLE 4.—MATERIALS COMBINATIONS

Non-oxide	Al_2O_3	SiO_2
Nb	✓	✓
Ta	✓	✓
Mo	✓	✓
W	✓	✓
Re	✓	✓
C	✓	✓

5.1.1 Phase diagram determinations of compatibility.—The quickest method to determine the possibility of reaction is to examine the Al-M-O or Si-M-O ternary phase diagram. The presence of a tieline between the metal and the oxide immediately tells one the two phases are compatible. In some cases these ternary phase diagrams are readily available; in other cases they are not available. This is summarized in table 5 below.

TABLE 5.—RELEVANT TERNARY PHASE DIAGRAMS

Ternary system	Isothermal cut available at temperature	Reference	Comments
Al-Nb-O	No	--	
Al-Ta-O	No	--	
Al-Mo-O		20	Mo-Al_2O_3 psuedo-binary indicates no reaction
Al-W-O	No	--	
Al-Re-O	No	--	
Al-C-O	25, 2127 °C	21	Compatible at room T, not at higher T
		--	
Si-Nb-O	No	--	
Si-Ta-O	700 to 1000 °C	22	Ta/SiO_2 Not compatible
Si-Mo-O	700 to 1000 °C	23	Mo/SiO_2 Compatible
Si-W-O	700 to 1000 °C	24	W/SiO_2 Compatible
Si-Re-O	No	--	
Si-C-O	1777, 1827 °C	25	C/SiO_2 Not compatible

The available phase diagrams are reproduced below. Figure 16(a) shows the pseudo-binary diagram for Mo-Al_2O_3. Clearly Mo is stable in contact with Al_2O_3.

Figure 16(b) is the Al-C-O ternary at 2127 °C. Note there is not a tie-line between C and Al_2O_3. In general oxides are not stable in contact with carbon at elevated temperatures, due to the high stability of the CO(g) product phase. Thus graphite should not be in contact with a sapphire crystal.

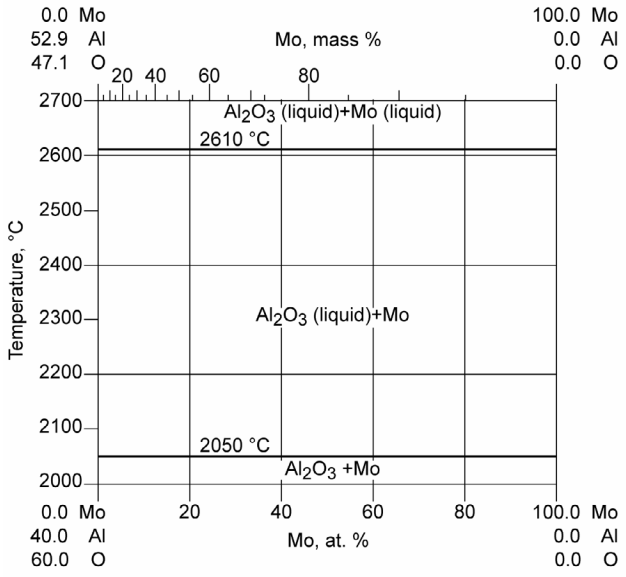

Figure 16(a).—Mo-Al_2O_3 psuedo-binary phase diagram (20).

Figure 16(a).—Mo-Al_2O_3 psuedo-binary phase diagram (ref. 20).

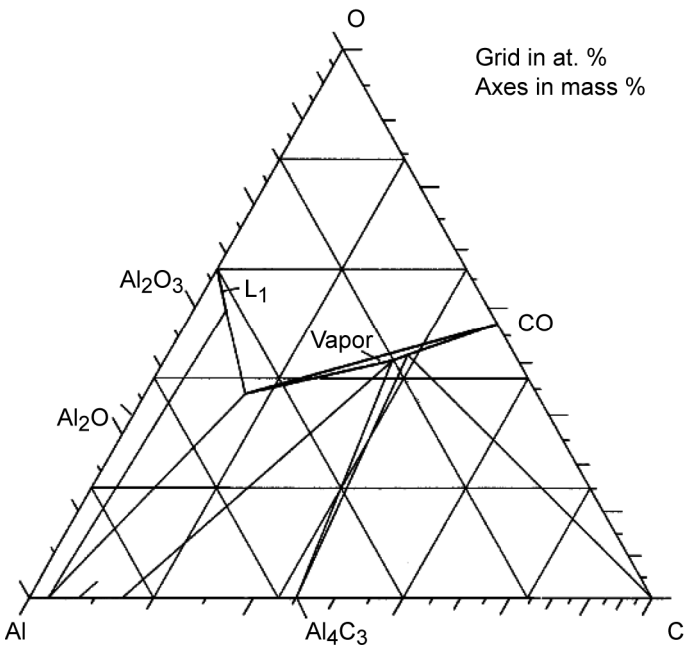

Figure 16(b).—Al-C-O section at 2127 °C (ref. 21).

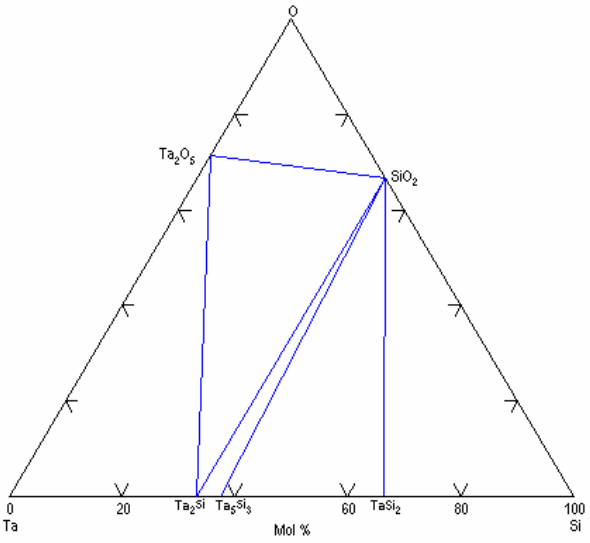

Figure 17(a).—Si-Ta-O ternary phase diagram (ref. 22).

Figure 17(a), (b), and (c) show the ternary phase diagrams for the Si-Ta-O, Si-Mo-O, and Si-W-O systems, respectively. There is no tieline between Ta and SiO_2, indicating that these two phases are not stable together. However the tieline between Mo and SiO_2 and the tieline between W and SiO_2 indicates that these two phases are stable together.

The diagrams shown above are calculated and are likely incomplete. One important feature, which is difficult to calculate, is the solubility of oxygen in the metallic phase. The solubility of oxygen in Mo is very low; however the solubility of oxygen in Nb is high (~9 a/o at 1915 °C). So it is likely that Nb would dissolve some oxygen when it is in contact with Al_2O_3 or SiO_2. This is best determined by experiment.

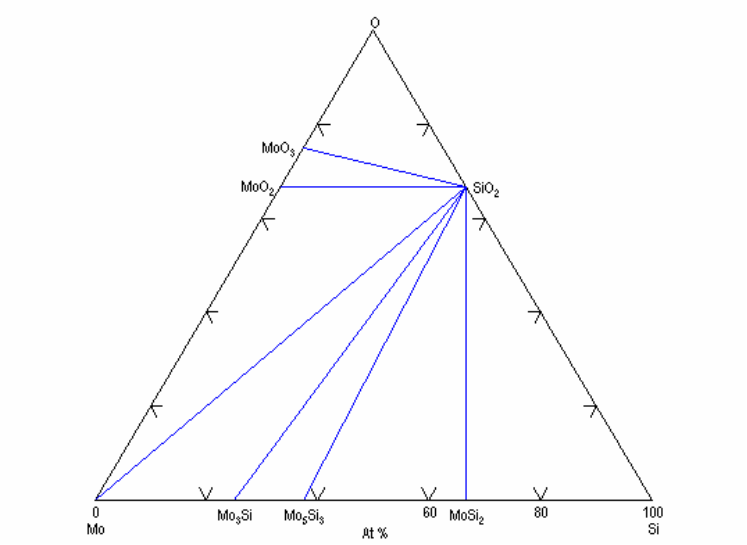

Figure 17(b).—Si-Mo-O ternary phase diagram (ref. 23).

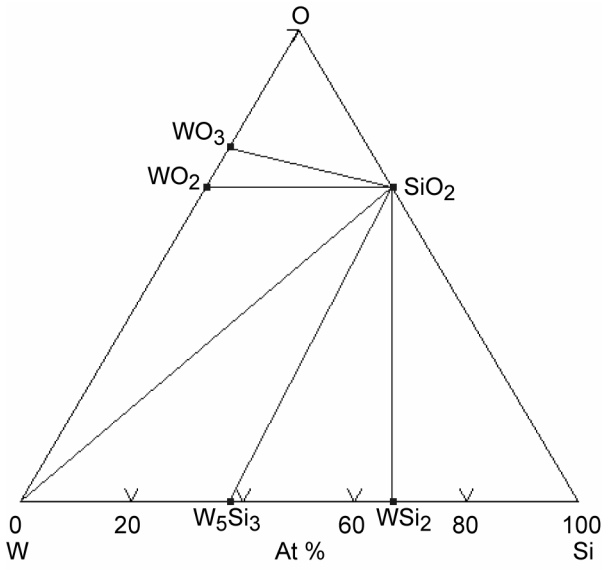

Figure 17(c).—Si-W-O phase diagram (ref. 24).

5.1.2 Generation of volatile species at the refractory metal/oxide interface.—Even though Mo and SiO_2 may not form another solid phase when placed in contact at elevated temperatures, they may generate some small amounts of volatile species. For example, it is known that SiO(g) and MoO_3(g) are stable gaseous species. Table 6 lists the results for each of the refractory metal/oxide combinations and the partial pressures of the major vapor species generated. A perfect vacuum was assumed and the vapor species listed were generated only from the interfacial reaction. In practice, other factors would play a role such as the background oxygen pressure discussed in section 4. However table 6 provides a way to rank the compatibility of the various refractory metals with sapphire and silica. These data are summarized in figure 18. For sapphire, it appears the least amount of vapor species are generated with Mo, W or Re. For silica, it appears that Mo, W or Re also generate the least amount of volatile species; however more vapor species are generated with silica than sapphire. Experiments need to be done to confirm this.

TABLE 6.—PREDICTED VAPOR PRESSURES FOR VARIOUS REFRACTORY METAL/OXIDE COMBINATIONS (Continued)

Metal/Oxide	Temperature, (K)	Pressure (bar) of vapor phase products
Nb/Al_2O_3	1000	$P(Products) < 1\times10^{-20}$
	1500	$P(Al) = 1.59\times10^{-11}$ $P(NbO_2) = 2.50\times10^{-12}$ $P(NbO) = 1.00\times10^{-12}$ $P(Al_2O) = 1.21\times10^{-13}$
	2000	$P(Al) = 6.74\times10^{-7}$ $P(NbO_2) = 5.12\times10^{-7}$ $P(NbO) = 1.54\times10^{-7}$ $P(Al_2O) = 8.27\times10^{-8}$
Ta/Al_2O_3	1000	$P(Products) < 1\times10^{-20}$
	1500	$P(Al) = 9.78 \times 10^{-12}$ $P(TaO_2) = 6.61\times10^{-12}$ $P(TaO) = 1.59\times10^{-12}$ $P(Al_2O) = 6.30\times10^{-14}$
	2000	$P(Al) = 7.62\times10^{-7}$ $P(TaO_2) = 5.95\times10^{-7}$ $P(TaO) = 1.51\times10^{-7}$ $P(Al_2O) = 9.74\times10^{-8}$
Mo/Al_2O_3	1000	$P(Products) < 1\times10^{-20}$
	1500	$P(Al) = 4.38\times10^{-14}$ $P(MoO) = 3.01\times10^{-14}$ $P(O) = 2.34\times10^{-14}$ $P(MoO_2) = 5.90\times10^{-15}$
	2000	$P(Al) = 1.44\times10^{-8}$ $P(MoO) = 1.15\times10^{-8}$ $P(O) = 3.71\times10^{-8}$ $P(MoO_2) = 3.62\times10^{-9}$
W/Al_2O_3	1000	$P(Products) < 1\times10^{-20}$
	1500	$P(O) = 3.54\times10^{-14}$ $P(Al) = 2.35\times10^{-14}$ $P(AlO) = 6.35\times10^{-16}$ $P(O_2) = 7.71\times10^{-17}$ $P(WO_2) = 2.59\times10^{-17}$
	2000	$P(O) = 7.45\times10^{-9}$ $P(Al) = 5.06\times10^{-9}$ $P(AlO) = 8.87\times10^{-10}$ $P(WO_2) = 1.57\times10^{-10}$ $P(O_2) = 1.26\times10^{-10}$
Re/Al_2O_3	1000	$P(Products) < 1\times10^{-20}$
	1500	$P(O) = 3.54\times10^{-14}$ $P(Al) = 2.35\times10^{-14}$ $P(AlO) = 6.35\times10^{-16}$ $P(O_2) = 7.72\times10^{-17}$ $P(Al_2O) = 2.03\times10^{-17}$ $P(ReO) = 1.30\times10^{-17}$

TABLE 6.—PREDICTED VAPOR PRESSURES FOR VARIOUS REFRACTORY METAL/OXIDE COMBINATIONS (Concluded)		
Metal/Oxide	Temperature, (K)	Pressure (bar) of vapor phase products
	2000	$P(O) = 7.62\times10^{-9}$ $P(Al) = 4.89\times10^{-9}$ $P(AlO) = 8.77\times10^{-10}$ $P(O_2) = 1.31\times10^{-10}$ $P(Al_2O) = 1.16\times10^{-10}$ $P(ReO) = 3.54\times10^{-11}$
C/Al_2O_3	Solid phases not compatible	
Nb/SiO_2	1000	$P(Products) < 1\times10^{-20}$
	1500	$P(SiO) = 4.30\times10^{-6}$ $P(NbO_2) = 1.53\times10^{-11}$ $P(Si_2O_2) = 1.28\times10^{-11}$ $P(SiO_2) = 7.53\times10^{-12}$ $P(NbO) = 1.00\times10^{-12}$
Ta/SiO_2	Solid phases not compatible	
Mo/SiO_2	1000	$P(Products) < 1\times10^{-20}$
	1500	$P(SiO) = 3.46\times10^{-9}$ $P(MoO_3) = 1.03\times10^{-9}$ $P(MoO_2) = 1.32\times10^{-10}$ $P(Mo_2O_6) = 1.57\times10^{-11}$
W/SiO_2	1000	$P(Products) < 1\times10^{-20}$
	1500	$P(SiO) = 4.25\times10^{-9}$ $P(W_2O_6) = 6.06\times10^{-10}$ $P(W_3O_9) = 4.15\times10^{-11}$ $P(W_3O_8) = 2.62\times10^{-11}$
Re/SiO_2	1000	$P(Products) < 1\times10^{-20}$
	1500	$P(SiO) = 7.10\times10^{-10}$ $P(ReO_3) = 2.18\times10^{-10}$ $P(O_2) = 1.78\times10^{-11}$ $P(O) = 1.70\times10^{-11}$ $P(SiO_2) = 7.53\times10^{-12}$ $P(ReO_2) = 6.73\times10^{-13}$
C/SiO_2	Solid phases not compatible	

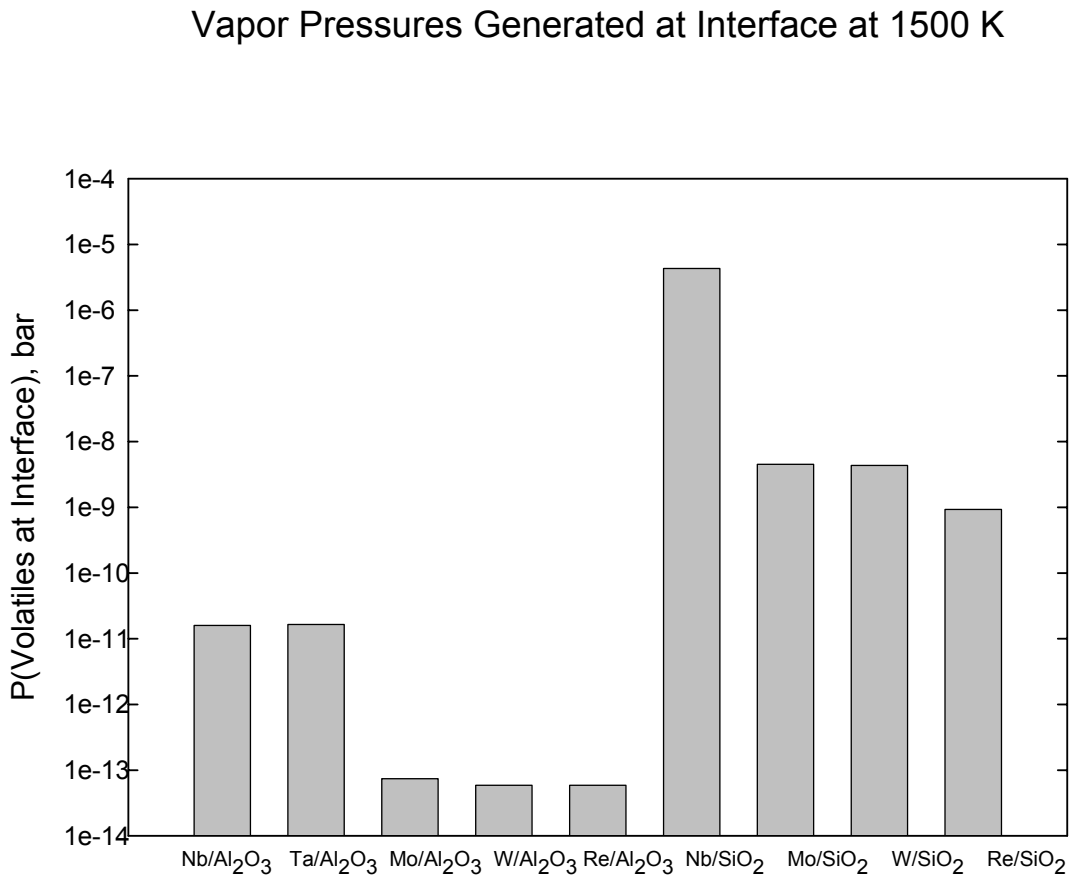

Figure 18.—Vapor pressures generated at refractory metal/oxide interfaces at 1500 K.

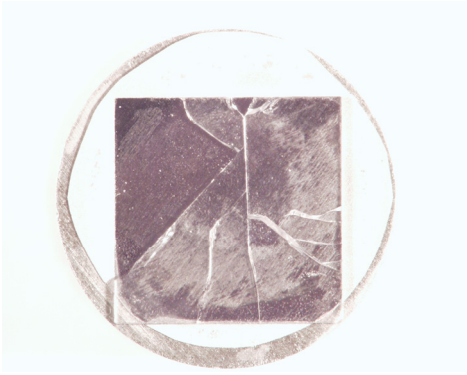

Figure 19.—Molybdenum and sapphire after hot press run at 1700 °C for 2 hr.

5.2 Experiments: Sapphire Compatibility

5.2.1 Experimental: sapphire+carbon.—In this case most of the sapphire reacted with the carbon (in the form of Graphoil®) to form a vapor. The chemical thermodynamic code FactSage (ref. 10) predicts that at 1700 °C, Al_2O_3 and C react to form CO at 0.125 atm, $Al_2O(g)$ at 6.2×10^{-3} atm, and Al(g) at 3.05×10^{-4} atm. In a vacuum, these products are removed and the reaction can go to near completion as was observed.

5.2.2 Experimental sapphire+molybdenum.—In this case the sapphire did not appear to react with the molybdenum. The molybdenum was cracked (fig. 19), but otherwise unreacted.

5.3 Experiments: Outgassing of Insulating Ceramics

Two insulating ceramics were tested for high temperature durability in preparation for the test of March 31, 2004. The first material is a fused silica foam (310M), available from Cotronics of Brooklyn, New York. It was cut in a 1 cc block and heated in the vacuum hot press furnace under the conditions listed in table 7. Note that even though there is 7 to 14 percent shrinkage in each direction, the weight changes are small. To see if the shrinkage was a one-time event, we ran the first sample twice. Shrinkage was substantially less, but a crack appeared. This crack appeared to be partially filled with a solidified glass-like substance. It may be that melting of one of the phases of this material limits its upper temperature to near 1649 °C (3000 °F). The 1 hr bake out at 1704 °C (3100 °F) did not lead to much more outgassing than the bake out at 1649 °C (3000 °F), but did lead to non-uniform shrinkage. The 2 hr bake out at 1704 °C (3100 °F) led to more uniform shrinkage and also the largest weight loss. The run at 1316 °C (2400 °F), repeated at 1649 °C (3000 °F) indicates that the lower temperature was insufficient to bake out the foam.

TABLE 7.—OUTGASSING AND SHRINKAGE OF SILICA FOAM MACHINEABLE CERAMIC ON VACUUM HEAT TREATMENT

Test date	Sample	T(C)/T(F)	Hold time		Length, (cm)	Width, (cm)	Height, (cm)	Weight, (mg)
2/3/2004	310M	1649/3000	1 hr	**Before**	1.090	1.082	0.933	0.86767
				After	0.958	0.933	0.821	0.85871
				% Change	–12.110	–13.771	–12.004	–1.033
3/1/2004	310M	1649/3000	1 hr	**Before**	0.958	0.933	0.818	0.85870
	again			**After**	0.958	0.936	0.826	0.85137
				% Change	0.000	0.322	0.978	–0.854
2/4/2004	310M	1704/3100	1 hr	**Before**	1.086	1.018	0.979	0.86560
				After	0.933	0.949	0.855	0.84419
				% Change	–14.088	–6.778	–12.666	–2.473
2/12/2004	310M	1704/3100	2 hr	**Before**	1.081	1.145	0.922	0.86317
				After	0.936	0.995	0.796	0.82973
				% Change	–13.414	–13.100	–13.666	–3.874
3/3/2004	310M	1316/2400	1 hr	**Before**	5.308	4.069	2.768	38.1611
				After	5.090	3.905	2.660	38.1475
				% Change	–4.107	–4.030	–3.902	–0.036
3/4/2004	310M	1649/3000	1 hr	**Before**	5.090	3.905	2.660	38.1475
	again			**After**	4.921	3.793	2.551	37.9759
				% Change	–3.320	–2.868	–4.098	–0.450

TABLE 8.—OUTGASSING AND SHRINKAGE OF MOLDABLE CERAMIC INSULATION ON VACUUM HEAT TREATMENT

2/24/2004	372UHT	1649/3000	2 hrs	**Before**	0.873	0.938	0.405	0.26997
				After	0.815	0.866	0.337	0.15113
				% Change	–6.644	–7.676	–16.790	–44.020
repeat								
2/26/2004	372UHT	1649/3000	2 hrs	**Before**	0.815	0.866	0.337	0.15091
				After	0.813	0.863	0.335	0.15072
				% Change	–0.245	–0.346	–0.593	–0.126

Table 8 shows the effect of vacuum heat treatment on a higher temperature "moldable" insulation (UHT272) containing ~98 percent Al_2O_3 and 2 percent SiO_2, also available from Cotronics of Brooklyn, New York. Note the extensive weight loss on a 1649 °C (3000 °F) treatment, which is part of the insulating molding to the part. Some of the weight loss is due to moisture, but other species may be released as well. As with the first material, we ran a repeat exposure and found considerably less shrinkage and weight loss.

Although these ceramic insulation materials are attractive as a holder for the crystal, the shrinkage and outgassing is an important issue to consider. Dimensional shrinkage must be accounted for in the design or the ceramic must be heat treated to the point where no more shrinkage is likely to occur. Outgassing is a more insidious problem. Generally outgassing is due to the release of adsorbed water. Water is an oxidant and has the same effect as oxygen on the refractory metals, discussed in section 4. Indeed, with water vapor, even higher vapor pressure metallic species may be produced due to some highly stable refractory volatile metal hydroxides (ref. 26). Therefore it is essential to thoroughly outgas these materials before use, as was done before the 2004 test.

6. Conclusions and Recommendations

The single crystal solar RSC is an exciting concept for conversion of sunlight to useful energy. However there are many challenges in bringing such a concept to reality. Most of these center on materials issues—particularly the stability of the RSC. As the crystal is heated and cooled, issues such as thermomechanical stability, thermochemical stability, and maintaining optical properties must be considered. Thermomechanical stability is a major issue and has been covered in another report (ref. 2). In a large crystal with a non-zero coefficient of thermal expansion, non-uniform temperatures will lead to stresses, which in could lead to failure in a crystal with stress concentrators, such as surface defects. In this report we focus on thermochemical stability—vaporization and reactions with support materials. Maintenance of optical properties is, of course, a critical issue. Some crystals are subject to solarization—discoloration from creation of color centers by UV radiation. Candidate materials must be tested for solarization and UV hardened if necessary.

At this point the two candidate materials are sapphire and vitreous silica. Sapphire has a higher temperature capability, but the results to date indicate many challenges in its application. Care must be taken to minimize stress concentrators from fabrication and thermal stresses in testing. Sapphire is also susceptible to solarization.

At this point, vitreous silica is suggested for a demonstration. Temperatures must be limited to less than ~1200 °C with this material due to devitrification, but it should not have the problems with thermal stresses. Vitreous silica samples also need to be tested for solarization susceptibility. A series of coupon tests on vitreous silica are suggested to check for the various issues discussed here—volatility, devitrification, solarization, and interfacial reactions—and to establish clear operating limits.

The solar/thermal RSC involves other high temperature materials, such as refractory metals and ceramic insulation. The behavior of these materials is also discussed. The problem with refractory metals (Nb, Ta, Mo, W, and Re) and carbon (C) is their reactivity with even small amount (~1 ppm = 10^{-6} atm) of oxygen. This can arise from outgassing of insulating materials and/or the soft vacuum of space. Thus the use of refractory metals requires a very low oxygen potential, which can be attained with either better pumping or an oxygen getter. As noted, proposed ceramic insulation materials outgas and shrink on first heating. This may be a source of oxidizing gases and these materials need to be thoroughly outgassed before use.

7. References

1. W.A. Wong and R.P. Macosko, "Refractive Secondary Concentrators for Solar Thermal Applications" Paper Number 99–01–2678 from the Proceedings of the 34th Intersociety Energy Conversion Engineering Conference, 1999. Also NASA/TM—1999-209379.
2. J.A. Salem, "Failure Analysis of the Second, Sapphire Solar Secondary Refractive Concentrator," NASA TM to be published.
3. J.A. Soules, D.R. Buchele, C.H. Castle, and R.P. Macosko, "Design and Fabrication of a Dielectric Total Internal Reflecting Solar Concentrator and Associated Flux Extractor for Extreme High Temperature (2500 K) Applications," NASA CR 204145, 1997.
4. S.M. Geng and R.P. Macosko, "Transient Thermal Analysis of a Refractive Secondary Solar Concentrator," Paper No. 1999–01–2680, 34th Intersociety Energy Conversion Engineering Conference Proceedings, Vancouver, British Columbia, Canada, August 1–5, 1999. Also NASA/TM—1999-209384.
5. W.A. Wong, S.M. Geng, C.H. Castle, and R.P. Macosko, "Design, Fabrication and Test of a High Efficiency Refractive Secondary Concentrator for Solar Applications" Paper Number AIAA–2000–2998 from the Proceedings of the 35th Intersociety Energy Conversion Engineering Conference, 2000. Also NASA/TM—2000-210339.
6. W.A. Wong and C.H. Castle, "High Temperature Solar Vacuum Testing of a Sapphire Refractive Secondary Concentrator" Proceedings of the Space Technology and Applications International Forum-STAIF 2002. American Institute of Physics Conference Proceedings, Vol. 608.
7. D. Jenkins, R. Winston, J. Bliss, J. O'Gallagher, A. Lewandowski, and C. Bingham, "Solar Concentration of 50,000 Achieved with Output Power Approaching 1 kW," J. Solar Energy Eng. 118, 141–45 (1996).
8. J. Karni, A. Kribus, P. Doron, A. Fiterman, and D. Sagie, "The DIAPR: A High-Pressure, High-Temperature Solar Receiver," J. Solar Energy Eng. 119, 74–78 (1997).
9. H. Ries, A. Segal, and J. Karni, "Extracting concentrated guided light," App. Optics 36 [13], 2869–74 (1997).
10. C.W. Bale, P. Chatrand, S.A. Degterov, G. Eriksson, K. Hack, R. Ben Mahfoud, J. Melancon, A.D. Pelton, and S. Peterson, "FactSage Thermochemical Software and Databases," CALPHAD 26 [2], 189–228 (2002).
11. H.A. Wang, C.H. Lee, F.A. Kröger, and R.T. Cox, "Point defects in α-Al_2O_3: Mg studied by electrical conductivity, optical absorption, and ESR," Phys. Rev. B 27 [6], 3821–3841 (1983).
12. John Emmett, Brush Prairie, WA, private communication.
13. David Joyce, Crystal Systems, Incorporated, Salem, MA, private communication.
14. D. Zhu, N.S. Jacobson, and R.A. Miller, "Thermal-Mechanical Stability of Single Crystal Oxide Refractive Concentrators for High-Temperature Solar Thermal Propulsion," Proceedings of Renewable and Advanced Energy Systems for the 21th Century (ed. by R. Hogan, Y. Kim, S. Kleis, D. O'Neal, and T. Tanaka), April 11–15, 1999, Maui, HI, ASME International, New York, NY.

15. S. Geng and J. Palko, unpublished work.
16. J.B. Lambert and J.J. Rausch, “Refractory Metals and Alloys,” in ASM Handbook, Vol. 2, ASM On-Line Books, December 1999.
17. N.S. Jacobson, D.L. Myers, D. Zhou, and D.L. Humphrey, “Rhenium/Oxygen Interactions at Elevated Temperatures,” Oxid. Met. 25 [5/6], 471–80 (2001).
18. N.J. Shaw, J.A. DiCarlo, N.S. Jacobson, S.R. Levine, J.A. Nesbitt, H.B. Probst, W.A. Sanders, and C.A. Stearns, “Materials for Engine Applications Above 3000 °F—An Overview,” NASA TM–100169, October 1987.
19. H. Yokokawa, “Understanding Materials Compatibility,” Annu. Rev. Mater. Res. 33, 581–610, 2003.
20. G. Petzow and G. Effenberg, Eds., “Ternary Alloys A Comprehensive Compendium of Evaluated Constitutional Data and Phase Diagrams,” Vol. 7, VCH Weinheim, Germany, 1993, 219–220.
21. G. Petzow and G. Effenberg, Eds., “Ternary Alloys A Comprehensive Compendium of Evaluated Constitutional Data and Phase Diagrams,” Vol. 3, VCH Weinheim, Germany, 1993, 525–533.
22. ACerS—NIST Phase Equilibria Diagrams, CD-ROM Database, Version 3.0, Figure 09163.
23. ACerS—NIST Phase Equilibria Diagrams, CD-ROM Database, Version 3.0, Figure 09160.
24. ACerS—NIST Phase Equilibria Diagrams, CD-ROM Database, Version 3.0, Figure 09165.
25. ACerS—NIST Phase Equilibria Diagrams, CD-ROM Database, Version 3.0, Figure 08697A-C.
26. N. Jacobson, D. Myers, E. Opila, and E. Copland, “Interactions of water vapor with oxides at elevated temperatures,” J. Phys. Chem. Solids 66, 471–478 (2005).

REPORT DOCUMENTATION PAGE

Form Approved
OMB No. 0704-0188

1. AGENCY USE ONLY (*Leave blank*)	2. REPORT DATE	3. REPORT TYPE AND DATES COVERED
	May 2005	Technical Memorandum

4. TITLE AND SUBTITLE

Materials Chemistry Issues in the Development of a Single Crystal Solar/Thermal Refractive Secondary Concentrator

5. FUNDING NUMBERS

WBS–22–972–30–03

6. AUTHOR(S)

Nathan S. Jacobson and Robert C. Biering

7. PERFORMING ORGANIZATION NAME(S) AND ADDRESS(ES)

National Aeronautics and Space Administration
John H. Glenn Research Center at Lewis Field
Cleveland, Ohio 44135–3191

8. PERFORMING ORGANIZATION REPORT NUMBER

E–15109

9. SPONSORING/MONITORING AGENCY NAME(S) AND ADDRESS(ES)

National Aeronautics and Space Administration
Washington, DC 20546–0001

10. SPONSORING/MONITORING AGENCY REPORT NUMBER

NASA TM—2005-213625

11. SUPPLEMENTARY NOTES

Nathan S. Jacobson, NASA Glenn Research Center; and Robert C. Biering, Analex Corporation, 1100 Apollo Drive, Brook Park, Ohio 44142. Responsible person, Nathan S. Jacobson, organization code RMD, 216–433–5498.

12a. DISTRIBUTION/AVAILABILITY STATEMENT

Unclassified - Unlimited
Subject Categories: 23 and 20

Available electronically at http://gltrs.grc.nasa.gov
This publication is available from the NASA Center for AeroSpace Information, 301–621–0390.

12b. DISTRIBUTION CODE

13. ABSTRACT ***(Maximum 200 words)***

The proposed solar/thermal Refractive Secondary Concentrator (RSC) is an advanced concept for converting sunlight to useful energy. A translucent crystal concentrates and transmits energy to a heat exchanger, which in turn heats a propellant gas, working gas of a dynamic power system, or a thermopile. Materials are the limiting issue in such a system. Central is the durability of the crystal, which must maintain the required chemical, physical/optical, and mechanical properties as it is heated and cooled. This report summarizes available data to date on the materials issues with this system. We focus on the current leading candidate materials, which are sapphire (Al_2O_3) for higher temperatures and silica (SiO_2) for lower temperatures. We use data from thermochemical calculations; laboratory coupon tests with silica and sapphire; and system tests with sapphire. The required chemical properties include low-vapor pressure and interfacial stability with supporting structural materials. Optical properties such as transmittance and index of refraction must be maintained. Thermomechanical stability is a major challenge for a large, single-crystal ceramic and has been discussed in another report. In addition to the crystal, other materials in the proposed system include refractory metals (Nb, Ta, Mo, W, and Re), carbon (C), and high-temperature ceramic insulation. The major issue here is low levels of oxygen, which lead to volatile refractory metal oxides and rapid consumption of the refractory metal. Interfacial reactions between the ceramic crystal and refractory metal are also discussed. Finally, high-temperature ceramic insulating materials are also likely to be used in this system. Outgassing is a major issue for these materials. The products of outgassing are typically reactive with the refractory metals and must be minimized.

14. SUBJECT TERMS

Space power; Space propulsion; Solar power; Materials; Chemistry; Thermodynamics

15. NUMBER OF PAGES

38

16. PRICE CODE

17. SECURITY CLASSIFICATION OF REPORT	18. SECURITY CLASSIFICATION OF THIS PAGE	19. SECURITY CLASSIFICATION OF ABSTRACT	20. LIMITATION OF ABSTRACT
Unclassified	Unclassified	Unclassified	